RSC Advances

PAPER

View Article Online
View Journal | View Issue

Cite this: *RSC Adv.*, 2026, **16**, 20241

Rhenium-186-labeled *ortho*-hydroxythiobenzhydrazide: a potential theranostic agent for use in metastatic breast cancer

Arpit Mitra,†[a] Avik Chakraborty, †[bf] Trupti Upadhye,[b] Sudeep Sahu,[b] Megha Tawate,[bf] Sudipta Chakraborty,[cf] Rubel Chakravarty, [cf] K. V. Vimalnath,[cf] Somnath Kar,[bf] Dolan Sengupta,[d] Snigdha Gangopadhyay,[e] Sanchita Goswami,[e] Pijush Kanti Gangopadhyay[e] and Sharmila Banerjee *[bf]

In this study, the aromatic thiobenzhydrazide derivative *o*-hydroxythiobenzhydrazide [H(htbh)] was radiolabeled with Rhenium-186 (^{186}Re) [$t_{1/2}$: 3.77 days, β_{max}: 1.07 MeV (71%), γ: 137 keV (9.47%)], produced in an in-house research reactor, yielding the [^{186}Re]Re-(htbh)$_2$ complex. The radiochemical purity (RCP) of the complex was found to be (98.07 ± 0.40)%. Mass spectroscopic analyses were used to elucidate the probable structure of the complex. The tumour targeting specificity of [^{186}Re]Re-(htbh)$_2$ was preliminarily assessed through *in-vitro* and *in-vivo* studies in preclinical models. While *in-vitro* studies included cell binding and internalization assays using MCF-7 cell lines, *in vivo* studies involved biodistribution analyses in SCID mice bearing MCF-7 induced human breast cancer xenografts. The pharmacokinetics revealed significant and prolonged tumour uptake, with SPECT/CT imaging showing plasma clearance within 24 hours and minimal retention in the liver and bladder.

Received 17th October 2025
Accepted 2nd April 2026

DOI: 10.1039/d5ra07970e

rsc.li/rsc-advances

1 Introduction

Metastatic breast carcinoma (MBC) remains one of the most common malignancies in women worldwide. It is typically managed with surgery and chemotherapy,[1] while radiotherapy serves as an additional option. Radiotherapy may involve either external beam radiotherapy (EBRT) or internalized sources of radiation. The latter, referred to as radionuclide therapy or radiopharmaceutical therapy (RPT), employs molecular vectors tagged with therapeutic radioisotopes emitting β^- or α particles. RPT, has particularly shown promise in MBC patients with overexpression of the Human Epidermal Growth Factor Receptor 2 (HER-2).[2]

RPT offers several advantages over EBRT, primarily due to its systemic or locoregional delivery of cytotoxic radiation to cancer cells or their microenvironment, either directly or by using delivery vehicles.[3] Among RPT agents, β^- emitting radiopharmaceuticals are more widely applied in MBC than those tagged with α emitting particles.[4,5] Radioimmunotherapy (RIT) with radiolabeled monoclonal antibodies (MAbs), such as trastuzumab, has been explored using ^{131}I, ^{177}Lu, and ^{90}Y. Although ^{131}I (β_{max}: 606 keV, γ_{max}: 364 keV, $t_{\frac{1}{2}}$ 8.02 d) and ^{177}Lu (β_{max}: 497 keV, γ_{max}: 208 keV, $t_{\frac{1}{2}}$ 6.73 d) possess favourable nuclear decay properties, their relatively low β^- energies limit efficacy against HER-2 positive lesions.[6–8] Conversely, the use of ^{90}Y (β_{max}: 2.27 MeV, $t_{\frac{1}{2}}$ 64.1 h), a pure β^- emitter without γ photons poses limitations towards post-therapy imaging with [^{90}Y]Y-trastuzumab.[9] The short half-life of ^{90}Y and the high molecular weight of trastuzumab (142.5 kDa), which slows the clearance kinetics, further reduce the therapeutic efficacy in MBC radiotherapy.[10,11]

While radiolabeled monoclonal antibody fragments (MAbs) such as [^{177}Lu]Lu-(Fab)$_2$-trastuzumab exhibit reduced residence times,[12] their preparation requires cumbersome Fc-fragment removal from (Fab)$_2$, prior to coupling with the chelator moiety.[13] These agents have also remained largely confined only to preclinical evaluation.[14]

Although ongoing studies with radiolabeled nanobodies or affibodies show promise due to their reduced residence time and faster *in vivo* clearance, extensive preclinical studies are mandatory pre-requisites for their clinical translation.[15,16] An important consideration that limits the use of radiolabeled MAbs, (Fab)$_2$-MAbs, nanobodies, or affibodies, is the requirement of a bifunctional chelator molecule[17,18] for complexation with ^{177}Lu and ^{90}Y and also size exclusion chromatography-based purification, which are time consuming and cumbersome processes.[6] In the case of

[a]*Radiopharmaceuticals Laboratory, Board of Radiation and Isotope Technology, Vashi, Navi Mumbai, India*
[b]*Radiation Medicine Centre, Bhabha Atomic Research Centre, Parel, Mumbai 400 012, India. E-mail: banerjeesharmila2207@gmail.com; Fax: +91-22-24157098; Tel: +91-9821872112*
[c]*Radiopharmaceuticals Division, Bhabha Atomic Research Centre, Trombay, Mumbai, India*
[d]*Department of Chemistry, Dumdum Motijheel College, Kolkata, India*
[e]*Department of Chemistry, University of Calcutta, 92 Acharya Prafulla Chandra Road, Kolkata, India*
[f]*Homi Bhabha National Institute,Trombay, Mumbai, India*
† Equal contribution first authors.

^{131}I radiolabeled MAbs, radiolabeling requires a time consuming and complex iodination procedures.[19–21] More recently, the fragmented antibody NM-02 radiolabeled with [^{188}Re]ReO_4^- has reached clinical trials in HER-2 positive breast cancer patients, though significant renal and hepatic accumulation limits its therapeutic profile.[22]

To overcome such challenges, small molecules have emerged as attractive targeting agents in RPT for MBC patients. Heterocyclic scaffolds such as thiosemicarbazones and thiosemicarbazides are well-studied for their diverse biological activities,[23] including anticancer effects in leukemia,[24] cervical carcinoma, and histiocytic lymphoma.[25] Substituted derivatives bearing aryl, aroyl, and heteroaryl groups around the thiosemicarbazide scaffold, inhibit DNA topoisomerase IIα (DTII) and indoleamine-2,3-dioxygenase-1 (IDO1),[26] which are both upregulated in breast tumours. By disrupting DTII and IDO1, these derivatives induce apoptosis and autophagy in cancer cells.[27] The well-documented anticancer activity of heteroaryl compounds bearing a thiosemicarbazide scaffold provided the impetus to investigate the therapeutic potential of Rhenium-186 and Rhenium188 labelled aromatic thiohydrazide-based compounds [R–C(=S)–NH–NH_2][R–C(=S)–NH–NH_2][R–C(=S)–NH–NH_2]. These radionuclides were selected in view of their favourable β^- emission characteristics, with maximum β energies of 1.07 MeV for ^{186}Re and 2.12 MeV[27] for ^{188}Re, rendering them suitable candidates for targeted radiopharmaceutical therapy. The syntheses and characterization of the aromatic thiohydrazide compounds thiobenzhydrazide [H(tbh)], *o*-hydroxythiobenzhydrazide [H(htbh)], thiophen-2-thiohydrazide [H(tth)], and furan-2-thiohydrazide [H(fth)] have been reported earlier.[28] The spectral properties of the metal complexes formed by all four aromatic thiohydrazides with Fe(III), Co(III) and Mo(VI) have also been studied[28–30] and the antibacterial properties of H(tbh) and H(tth) have also been documented earlier.[29]

Inspired by these findings, we focused on aromatic thiohydrazides, owing to their structural similarity with thiosemicarbazides. Among them, *o*-hydroxythiobenzhydrazide (H(htbh)) has not yet been explored for its anticancer activity. The ligand H(htbh) possesses a phenolic hydroxyl group and a hydrazide moiety, enabling stable chelation with transition metals, a prerequisite for *in-vivo* stability and tumour targeting. Hydrazide derivatives also exhibit selective interactions with tumour-associated biomolecules, possibly *via* nucleophilic binding or receptor-mediated recognition.

The selection of Rhenium (Rhenium-186 or Rhenium-188) as the radioisotope was driven by the favourable disposition of the array of donor atoms present in the H(htbh) ligand, which are well-suited for complexation with Re(V). Incorporating a radioactive Re isotope into the H(htbh) framework could yield a stable radiometal complex with inherent tumour-targeting capability, enabling simultaneous imaging and targeted radiotherapy of metastatic breast cancer lesions. Given the lipophilic and chelating characteristics of H(htbh) derivatives, such complexes may demonstrate favourable pharmacokinetics, including enhanced tumour uptake and rapid clearance from non-target organs, reducing systemic toxicity. The radiolabeled H(htbh) complexes with NS-donor ligands are advantageous due to their lower molecular weight compared to radiolabeled monoclonal antibodies (MAbs), resulting in faster clearance kinetics.[31] The complexes with N and S donor groups are known to exhibit lipophilic properties.[32] Consequently, the rhenium labeled H(htbh) complex is expected to possess suitable lipophilicity, which is crucial for effective distribution and localization in overexpressed DTII and IDO1 enzymes in MBC patients.[27,33]

Pertinent to the field of radiopharmaceutical chemistry, Rhenium (Re) complexation of H(htbh) can be possible using either the precursor, [^{186}Re]ReO_4^- or [^{188}Re]ReO_4^-. While Re-186 is available as a radiochemical typically in the form of [^{186}Re]ReO_4^-, produced in the in-house research reactor (DHRUVA), at a thermal neutron flux of 3×10^{13} n cm^{-2} s^{-1}, [^{188}Re]ReO_4^- is available as a generator eluate from the commercial ^{188}W/^{188}Re generator. Both these Re radioisotopes possess nuclear decay characteristics consisting of γ photons enabling non-invasive monitoring through nuclear imaging modalities and a medium energy (Re-186) and high energy (Re-188) β^- particulate emission, offering cytotoxic effects on cancerous cells.[34–37] Thus, the development of a radioactive [$^{186/188}$Re]Re-(htbh)$_2$ complex holds promise as a dual-function theranostic agent for managing metastatic breast cancer, combining the possibility of targeted radiotherapy and diagnostic imaging within a single molecular platform.

The radiochemical precursor [$^{186/188}$Re]ReO_4^-, is expected to form stable complexes with [H(htbh)] in the (+5) oxidation state.[38] Our primary objective was to develop a stable formulation of [$^{186/188}$Re]Re-(htbh)$_2$ complex and carry out its characterization (physico-chemical, *in-vitro* and *in-vivo*, stability) as well as preclinical evaluation, in assessing its potential as a theranostic agent. In line with the envisaged strategy, aromatic thiohydrazide, [H(htbh)] was radiolabeled with medium specific activity, carrier added [^{186}Re]ReO_4^- with a view to optimizing the radiochemical synthesis of [^{186}Re]Re-(htbh)$_2$ for obtaining consistent and reliable radiochemical purity (RCP) of the complex. The quality control parameters of the [^{186}Re]Re-(htbh)$_2$ complex were thoroughly validated. Various *in-vitro* pharmacokinetic studies involving cell binding, cell internalization, flow cytometry and [3-(4,5-dimethylthiazolyl-2)-2,5-diphenyltetrazolium bromide)] assay (MTT assay) of the complex were carried out in breast cancer cell lines (MCF7). Its *in-vivo* pharmacological behaviour was studied in female SCID mice with MCF7 tumour xenografts. The results conclusively established the effectiveness of the [^{186}Re]Re-(htbh)$_2$ in targeting breast cancer. The specificity of the [^{186}Re]Re-(htbh)$_2$ complex in MBC was evaluated by carrying out various *in-vitro* pharmacokinetic and *in-vivo* pharmacological studies. The results reveal that [^{186}Re]Re-(htbh)$_2$ could be effectively used to target high-capacity receptor overexpression, particularly in cases of metastatic breast carcinoma.[22]

The *in-vivo* distribution was examined in female SCID mice with MCF7 tumour xenografts; using SPECT/CT based static imaging, at 1 h post injection (p.i). The preclinical study of the [^{186}Re]Re-(htbh)$_2$ complex reported herein, provides confirmatory indications towards its potential as a theranostic agent for targeting breast cancers. The strategy envisaged is to extrapolate the present findings towards the development of a [^{188}Re]ReO_4^- based therapeutic agent having comparatively higher β_{max} (2.12

MeV) compared to that of [^{186}Re]ReO_4^-, with potential application in targeted radiotherapy of MBC.

2 Experimental

2.1 Materials

2-hydroxy thiobenzhydrazide [H(htbh)] used in this studies was custom synthesized as per reported procedure.[28,29] Enriched target (^{185}Re metallic powder, enrichment > 95%, purity > 99.999%) used for irradiation, was obtained from Isoflex, Russia. Stannous chloride dihydrate ($SnCl_2 \cdot 2H_2O$) was purchased from Sigma-Aldrich, USA. HCl (30%, Ultrapur®), ethanol (Emsure), 2,5- dihydroxybenzoic acid (Gentisic acid, purity > 98%) and ammonium perrhenate (purity: 99.999% trace-metal basis) were procured from Merck, Germany. Polyethersulfone (PES, pore size: 0.22 μm) membrane syringe filter was procured from Millipore-Merck, Germany. Non-bleeding type pH indicator strips (range: 0–14) were from Merck, India. Sterile, pyrogen-free saline was procured from Nirlife Healthcare, India. Bio-safety cabinet (ISO Class 5) was purchased from Microfilt, India, while the fume hood (lead shielded) was from Labguard, India. Analytical radio-high performance liquid chromatography (radio-HPLC) was performed using HPLC system from Knauer, Germany, equipped with UV and radioactive detectors, connected in series. Radio-thin layer chromatography (radio-TLC) and radio paper chromatography (radio-PC) were performed using miniGita equipped with NaI(Tl) radioactive detector from Bioscan, USA. Radionuclide purity (RNP) of [^{186}Re]ReO_4^- obtained after radiochemical processing of reactor-irradiated targets was determined by gamma ray spectroscopy, using high-purity germanium (HPGe) detector (Baltic Scientific Instruments, Russia), coupled to 4 k and 64 k multichannel analyzer (MCA) (ITECH instruments, France). Dose calibrator (CRC 25R) was from Capintec, USA. Endotoxin limit (EL) was quantified by gel-clot BET assay method using LAL reagent from Charles River Laboratories Inc, USA, while the sterility test was performed by direct inoculation method using soya bean casein digest and fluid thioglycolate media from Himedia, India. *In-vitro* cell binding and internalization studies were carried out using human breast cancer cells MCF7 (ATCC®, HTB-22™). Media (IMDM), fetal bovine serum (FBS) and bovine serum albumin (BSA) for growing MCF7 cells were obtained from Gibco, Thermo Fisher Scientific USA. *In-vivo* distribution studies of [^{186}Re]Re-$(htbh)_2$ were carried out in female SCID mice aged 3 to 4 weeks [SCID-Beige mice (C.B-*Igh*-1b/GbmsTac-*Prkdc*^{scid}-*Lyst*^{bg} N7)] were procured from *Vivo* Biotech, India. Monkey kidney cell line (Vero cells) were procured from National Centre for Cell Science (NCCS), Pune, India. NaI(Tl) γ-counter was procured from Para Electronics, India. SPECT/CT imaging for SCID mice bearing tumour xenografts was carried out using NM/CT 870 DR from GE, Sweden.

2.2 Methods

2.2.1 Production and quality control of [^{186}Re]ReO_4^-. Enriched rhenium metallic powder (~10 mg, enrichment: >95%) was irradiated in the DHRUVA reactor, at a thermal neutron flux of 3×10^{13} n cm^{-2} s^{-1}, for 7 days *via* ^{185}Re(n,γ)^{186}Re nuclear reaction. The irradiated target after cooling for 4 days, was dissolved in 5 mL of 2 M HNO_3. The radiochemical separation and purification was carried out to obtain clinical grade Na[^{186}Re]ReO_4, as per our earlier reported procedure.[39] The specific activity of the clinical grade product, Na[^{186}Re]ReO_4 varied in the range of 9.99–10.28 GBq mg^{-1}.

The radionuclide purity (RNP) of the produced ^{186}Re was estimated by gamma ray spectroscopy. The assay of radionuclidic (RN) purity and radioactivity of $^{188/186}$Re formed were estimated by gamma ray spectrometry, using HPGe detector connected to a 4 K multichannel analyzer. ^{152}Eu standard source obtained from Amersham International (United Kingdom) was used for energy calibration of the instrument. An aliquot of the sample (37–74 KBq) was counted to estimate the percentages of ^{188}Re and ^{186}Re in the samples as well as any other RN impurities. The ^{188}Re and ^{186}Re were analysed using the 155 and 137 keV γ photo peaks, respectively.

The radiochemical purity (RCP) of the Na[^{186}Re]ReO_4 was assessed by radio-TLC and radio-PC using saline and radio-HPLC. The pH of the Na[^{186}Re]ReO_4 was determined by narrow range pH strip.

2.2.2 Radiolabeling of H(htbh) with Na[^{186}Re]ReO_4. Non-carrier-free Na[^{186}Re]ReO_4 (600 μL, specific activity: 10 GBq mg^{-1}, pH: 6.0) solution (1.6 GBq of [^{186}Re]ReO_4^-, 159 μg, 0.855 μmol Re) was acidified with 1 M HCl (150 μL), the resultant pH of [^{186}Re]ReO_4^- was 2.0. Acidified [^{186}Re]ReO_4^- (1.6 GBq) was then added to 1436 μL of H(htbh) ligand (1436 μg) (concentration: 1 μg μL^{-1} of solution in ethanol, 8.55 μmol, 10 equivalent of Re), containing 20 μL (1.96 mg, 8.67 μmole) of stannous chloride ($SnCl_2 \cdot 2H_2O$ dissolved in 30% HCl). The reaction was carried out in a boiling water bath (100 °C) for 4–5 minutes till the colorless reaction mixture changes to faint green color. The reaction mixture was cooled to room temperature (25 °C). On cooling, 5 mg of 2,5-dihydroxybenzoic acid (gentisic acid as a stabilizer for preventing radiolytic dissociation) in 1.0 mL of saline was added to the reaction mixture. The reaction mixture was further diluted with 11.8 mL of sterile, pyrogen-free saline (0.9% NaCl), in order that the radioactive concentration (RAC) and ethanol concentration was maintained at 107 MBq mL^{-1} and <10% v/v respectively in the final formulation. The concentration of 2,5-dihydroxybenzoic acid in [^{186}Re]Re-$(htbh)_2$ was found to be 3.1 mg GBq^{-1}. The final product [^{186}Re]Re-$(htbh)_2$, volume: 15 mL was filtered using sterile 0.22 μm PES membrane syringe filter.

2.2.3 Synthesis and chemical characterization of [^{185}Re]Re-$(htbh)_2$ complex. An aqueous solution of 0.5 mL of ammonium perrhenate (concentration: 20 mg mL^{-1} of solution in ethanol) containing 10 mg of ammonium perrhenate (54 μmole) was acidified with 1 M HCl, the resultant pH of NH_4[^{185}Re]ReO_4 was 1.0–2.0. The acidified NH_4[^{185}Re]ReO_4 was added to 2.28 mL (91 mg) of H(htbh) ligand (concentration: 40 mg mL^{-1} of solution in ethanol, 541 μmol, 10 equivalent of ammonium perrhenate) containing 60 μL (5.88 mg, 26.01 μmole) of stannous chloride ($SnCl_2.2H_2O$ dissolved in 30% HCl). The reaction was carried out in a boiling water bath (100 °C) for 4–5 minutes till a faint green color was observed. The non-radioactive reference

complex *i.e.* [^{185}Re]Re-(htbh)$_2$ was used in ethanol medium. The UV-HPLC of the non-radioactive [^{185}Re]Re- (htbh)$_2$ complex was carried out using Eurosphere C-18 reversed phase column {Dimension: 300 mm (Length) × 4 mm (Diameter), particle size: 5 μm}, equipped with diode array detector (DAD)-UV (wavelength set at 310 nm), using 0.1% TFA in water and acetonitrile as solvent system. The flow-rate was maintained at 0.5 mL min^{-1}, in gradient mode (0–1 min 95% water, 1–2 min 95% to 60% water, 2–5 min 60% to 75% water, 5–8 min 75% to 85% water, 8–12 min 85% to 95% water and 12–16 min 95% water). The non-radioactive reference complex [^{185}Re]Re-(htbh)$_2$ was synthesized in ethanol and characterized by UV-HPLC. The UV-HPLC chromatogram exhibited a single, well-defined peak at a retention time (R_t) of 3.20 min, confirming the formation of a single complex without detectable impurities. This retention time closely matched that of the radioactive analogue [^{186}Re]Re-(htbh)$_2$ (R_t = 3.33 min, radio-HPLC), thereby establishing the chemical equivalence of the non-radioactive and radioactive complexes. Ethanol was removed by rotary evaporation to obtain the complex in powder form for further characterization, by FT-IR, ^{1}H-NMR spectroscopy and high-resolution mass spectrometry (HRMS).

Mass spectroscopy analyses of [^{185}Re]Re-H(htbh)$_2$ complex was carried out in Agilent LCMS Spectrometer (LCMSQTOF-G6545B). ^{1}H-NMR spectroscopy was performed using Bruker Advance Neo (400 MHz) instrument. Atteneuated Total Reflection-Fourier Transform Infrared (ATR-FTIR) spectroscopy for [^{185}Re]Re-(htbh)$_2$ complex was carried out in Bruker Platinum ATR Tensor-II FT-IR spectrometer.

2.2.4 Quality control studies of [^{186}Re]Re-(htbh)$_2$. The pH of [^{186}Re]Re-(htbh)$_2$ was measured by observing the colour change (using narrow range pH strips on spotting 1–2 μL of the final product.

The radiochemical purity (RCP) of the [^{186}Re]Re-(htbh)$_2$ complex was initially assessed by radio-PC (Whatman 3 MM, thickness: 0.34 mm) using an ethanol/chloroform/benzene (1.5/2/1.5, v/v/v) solvent system. In addition, RCP was also evaluated by radio-TLC using saline and acetone as mobile phases. This additional assessment was undertaken because the ethanol/chloroform/benzene system did not provide clear separation of potential impurities such as [^{186}Re]ReO$_4^-$ and [^{186}Re]ReO$_2$ from the desired product, if present.

The RCP of [^{186}Re]Re-(htbh)$_2$ was also ascertained by radio-HPLC using Eurosphere C-18 Reversed phase column {Dimension: 300 mm (Length) × 4 mm (Diameter), particle size: 5 μm} equipped with diode array detector (DAD)-UV (wavelength set at 310 nm) and radioactive detectors [NaI(Tl)], connected in series, using 0.1% TFA in water and acetonitrile as solvent system. The flow-rate was maintained at 0.5 mL min^{-1} in gradient mode (0–1 min 95% water, 1–2 min 95% to 60% water, 2–5 min 60% to 75% water, 5–8 min 75% to 85% water, 8–12 min 85% to 95% water and 12–16 min 95% water).

2.2.5 Stability and transchelation studies of [^{186}Re]Re-(htbh)$_2$

2.2.5.1 Saline stability. The stability of the [^{186}Re]Re-(htbh)$_2$ complex, in saline. on storage at room temperature (25 °C), was evaluated by radio-HPLC up to 3 h post-radiolabeling.

2.2.5.2 Phosphate buffered saline (PBS) stability. In-vitro stability of the [^{186}Re]Re-(htbh)$_2$ complex was evaluated in PBS (pH: 7.4) by radio-HPLC. Towards this, [^{186}Re]Re-(htbh)$_2$ complex (~0.2 GBq in 100 μL) was incubated with 400 μL of PBS at 37 °C for 24 h. The stability of the [^{186}Re]Re-(htbh)$_2$ complex was evaluated by radio-HPLC, post 24 h of incubaton at 37 °C.

2.2.5.3 Serum stability. Towards assessing the serum stability, the [^{186}Re]Re-(htbh)$_2$ complex was incubated with the serum from healthy volunteers, at 37 °C for 3 h. Post incubation, serum proteins were precipitated (acetonitrile, RCF 3500 g), while serum samples were stored at −20 °C up to 18 h. The RCP of the serum samples was evaluated by radio-PC, post 18 h on storage at −20 °C.

2.2.5.4 Transchelation studies. Transchelation or ligand exchange studies of the [^{186}Re]Re-(htbh)$_2$ was carried out using diethylenetriaminepentaacetic acid (DTPA).

2.2.5.5 Control samples. The [^{186}Re]Re-(htbh)$_2$ complex (~0.2 GBq in 100 μL) was incubated with 400 μL of PBS, at 37 °C for 24 h.

2.2.5.6 Test samples. The [^{186}Re]Re-(htbh)$_2$ complex (~0.18 GBq, ^{186}Re: ~120 μg, ~0.64 μmoles) along with DTPA (25 mg, ~63.55 μmoles, ~100 equivalent of Re) was incubated with 400 μL of PBS at 37 °C for 24 h. Experiments were performed in triplicate.

Post-incubation at 37 °C for 24 h, RCP for the control and test samples were assessed by radio-HPLC.

Endotoxin limit (EL) was quantified by gel-clot BET assay method using lysate, with sensitivity 0.125 EU mL^{-1}, at 200 maximum valid dilution (MVD). The sterility testing of the [^{186}Re]Re-(htbh)$_2$ complex was carried out by direct inoculation method.

2.2.6 *In-vitro* pharmacokinetic studies of [^{186}Re]Re-(htbh)$_2$

2.2.6.1 Cell binding. Human breast cancer cell line MCF7 (ATCC®, HTB-22™) was used for *in-vitro* cell binding study for the evaluation of [^{186}Re]Re-(htbh)$_2$ complex. The cell line was grown in 6 well, tissue culture dish using IMDM medium supplemented with 10% FBS in 5% CO_2 at 37 °C, under humid condition. MCF7 cells (1×10^6 cells each) were subjected to [^{186}Re]Re-(htbh)$_2$ (0.1 pmole). The cells were incubated with the [^{186}Re]Re-(htbh)$_2$ complex, in cell binding buffer (IMDM with 0.2% BSA), for different time intervals (15, 30, 60 and 120 min). The incubation was followed by washing twice with ice cold 0.05 M phosphate buffered saline (PBS, pH 7.4) and centrifugation at 4000 rpm for 5 minutes. The cell pellet was then analyzed in a well-type NaI(Tl) scintillation gamma counter for determining the extent of total cell bound activity. The extent of non-specific binding (NSB) was confirmed by incubating the same number of cells and [^{186}Re]Re-(htbh)$_2$ with 100 nM of cold H(htbh). In brief, NSB was determined by performing the binding assay in the presence of an excess concentration (100 nM) of cold H(htbh), which competitively blocks the specific binding. Under these conditions, the remaining cell-associated radioactivity was considered to be non-specific binding. This competitive binding approach was employed to evaluate the specificity of interaction of H(htbh) with the cell line. Additionally, binding studies with monkey kidney cell line, Vero

cells were carried out under identical condition, in order to further ascertain the specificity of the [^{186}Re]Re-(htbh)$_2$. Each treatment was completed in triplicate ($n = 3$), with each experiment being repeated at least twice.

2.2.6.2 Cell internalization. For internalization studies, cells were incubated with [^{186}Re]Re-(htbh)$_2$ as described earlier. Following incubation, the culture medium was removed and the cells were washed twice with ice-cold PBS. The adherent MCF7 cells were detached using a high-concentration EDTA solution, as per standard protocol. To remove the surface-bound radioactivity, cells were subjected to an acid wash while remaining adherent to the culture plate, using 500 μL of acidic buffer (50 mM glycine, 100 mM NaCl, pH 2.8), for 5 min at 4 °C. The acidic buffer was then removed, and the cells were washed again with cold PBS to ensure complete removal of membrane-bound activity.

Subsequently, the cells were lysed using 500 μL of 1 N NaOH to release internalized radioactivity. All washing and lysis steps were performed at 4 °C to minimize membrane disruption and prevent artifactual internalization. The radioactivity associated with the cell lysate was measured using a NaI(Tl) gamma counter and considered as the internalized fraction.

2.2.6.3 MTT assay for assessment of cytotoxicity. The cytotoxic potential of [^{186}Re]Re-(htbh)$_2$ and cold H(htbh) were assessed using MTT assay[40] in MCF7 cell lines. Briefly, 1×10^4 cells per well were seeded in 96-well plates and incubated overnight. Cells were then exposed to increasing concentrations (5–40 μg mL^{-1}, expressed as ligand-equivalent mass) of H(htbh) and [^{186}Re]Re-(htbh)$_2$ for 2 h. Following exposure, the treatment medium was removed, cells were washed with PBS to eliminate unbound activity, and fresh culture medium was added. Cells were then incubated for an additional 24 h, after which cytotoxicity was assessed by the MTT assay. For radiolabeled samples, the corresponding radioactivity of ^{186}Re in [^{186}Re]Re-(htbh)$_2$ ranged from 0.1–0.2 MBq per well.

As [^{186}Re]Re-(htbh)$_2$ was dissolved in labeling buffer, the same buffer in the treatment groups was used as vehicle control. Cells were washed with PBS and incubated further for 3 h with 100 μL of 0.5 mg mL^{-1} of MTT. The formazan crystals formed were dissolved in 100 μL of 10% SDS for 2 h and absorbance was measured at 570 nm using a micro-plate spectrophotometer (iMax™, BioRad, USA). Each treatment was carried out in triplicate with each experiment being repeated at least twice. For the MTT assay, the relative cell viability (%) compared to the control cells was calculated using the following equation:

$$\text{Cell viability (\% of sample)} = (A_{\text{sample}}/A_{\text{control}}) \times 100,$$

where A_{sample} and A_{control} are the absorbance values obtained for cells treated with cold H(htbh) and [^{186}Re]Re-(htbh)$_2$ formulations and for cells incubated with the culture medium, respectively. Histogram was plotted as different formulations *versus* percent cell viability.

2.2.6.4 Flow cytometry analysis. The distribution of necrotic/apoptotic and live cells was tested using flow cytometry (CyFlow® Space, Sysmex, USA) method. Towards this, MCF7 cells were exposed to bare H(htbh) for 24 h with equivalent concentration (10 and 20 μg mL^{-1}). The cells were harvested and washed with cold PBS two times. The cells were fixed thereafter by addition of 80% ethanol and incubated at −20 °C for 24 h. After incubation the cells were removed and washed with ice cold PBS (1X). For determination of Sub G1 *i.e.* apoptotic cell population, cell pellets were collected by centrifugation and stained with 2 mL PI staining solution for 1 h, in dark (PI stain: D/W, containing 0.1% Triton X 100, 0.1% sodium citrate, 50 μg mL^{-1} PI and 50 μg mL^{-1} RNase A). For each experiment, at least 10 000 cells were counted. The DNA contents were analyzed by the FlowJo 5 Express software (*De Novo* Software, USA).[41,42]

2.2.7 *In-vivo* distribution studies of [^{186}Re]Re-(htbh)$_2$. Female SCID mice aged 3 to 4 weeks were used for the evaluation of *in-vivo* pharmacokinetics and bio-distribution [SCID-Beige mice (C.B-*Igh*-1b/GbmsTac-*Prkdc*^{scid}-*Lyst*^{bg}N7)]. MCF7 cells (2×10^6 cells per mice) were injected subcutaneously into the flank region of mice. The xenografts were allowed to grow for 6 weeks until the tumour attains the necessary size (volume: 1–1.5 cm^3). [^{186}Re]Re-(htbh)$_2$ (3.0–3.7 MBq per animal) were injected in xenografted mice through the tail vein. Post-injection, the *in-vivo* localization of the [^{186}Re]Re-(htbh)$_2$ were assessed at 0.5 h, 2 h and 24 h time intervals. Each experimental group consisted of three mice ($n = 3$). The accumulated radioactivity in the vital organs of the animals was measured, using a flat-bed NaI(Tl) gamma counter. Biodistribution data of accumulated activity for the organs were plotted as %ID g^{-1}. The organ/tumour ratio were plotted for major organs. The *in-vivo* distribution, 1 h post injection (p.i.) was examined by static imaging using a SPECT/CT camera (GE Medical, Sweden). All the biodistribution studies were carried out under Isoflurane-oxygen anesthesia, following the ethical guidelines for animal experimentation.[6] Studies were performed in SCID mice after obtaining regulatory clearance from the Institutional Animal Ethics Committee (IAEC) and in accordance with the guidelines set for conducting experimentation in laboratory animals.

2.2.8 Regulatory clearance aspects. All animal experiments were carried out with the prior approval of the Institutional Animal Ethics Committee (IAEC), Bhabha Atomic Research Centre (BARC), Department of Atomic Energy (DAE), Government of India, following the principle of good laboratory practices (GLP).

The protocol followed for carrying out serum stability study was approved by the Institutional Scientific and Medical Ethics Committee of the Radiation Medicine Centre, BARC and was conducted in accordance with the Declaration of Helsinki and Good Clinical Practice guidelines. Blood samples, required for serum extraction, were collected from healthy volunteers after obtaining their prior written informed consent.

3 Results

3.1 Radiolabeling of [^{186}Re]Re-(htbh)$_2$

The radiochemical precursor [^{186}Re]ReO$_4^-$, produced and processed in house, was used for radiolabeling of H(htbh) and 1.6 GBq of the complex [^{186}Re]Re-(htbh)$_2$ was prepared, ($n = 7$) with RCY (97.04 ± 0.49)%. The [^{186}Re]Re-(htbh)$_2$ complex was found

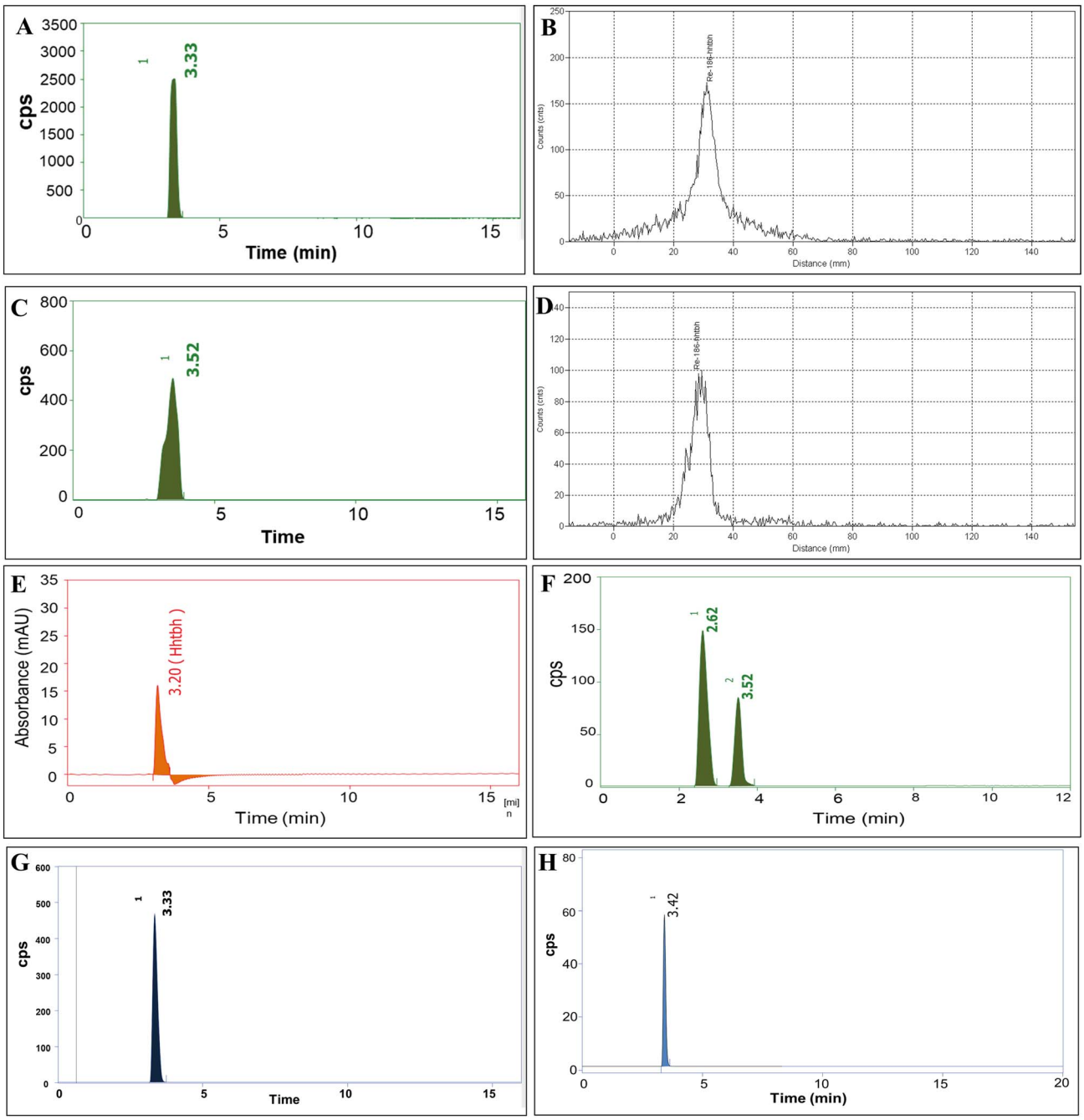

Fig. 1 Chromatograms of [^{186}Re]Re-(htbh)$_2$; (A) radio-HPLC (R_t: 3.33 min); (B) radio-PC (R_f: 0.59); (C) radio-HPLC (R_t: 3.52 min) at 3 h post radiolabeling, with stabilizer, on storage, at room temperature *i.e.* 25 °C in saline; (D) radio-PC (R_f: 0.52) after 3 h incubation (in healthy human serum, at 37 °C) & on further storage up to 18 h at −20 °C; (E) UV-HPLC chromatogram of non-radioactive [^{185}Re]Re-(htbh)$_2$ complex (R_t: 3.20 min); (F) radio-HPLC of [^{186}Re]Re-(htbh)$_2$ (R_t: 3.52 min) co-injected with Na[^{186}Re]ReO$_4$ (R_t: 2.62 min); (G) radio-HPLC (R_t: 3.33 min) at 24 h post incubation in PBS; (H) radio-HPLC of [^{186}Re]Re-(htbh)$_2$ (R_t: 3.42 min) at 24 h post incubation (37 °C) with 100 fold molar excess of DTPA.

to be clear being faint green in color, with pH in the range of 4.0–5.0, and RAC between ~107 MBq mL^{-1}. The maximum RCY was observed at a metal (M) : ligand (L) molar ratio of 1 : 10, where M is [^{186}Re]Re and the ligand is H(htbh).

3.2 Quality control studies of [^{186}Re]Re-(htbh)$_2$

The RCP of [^{186}Re]Re-(htbh)$_2$ ($n = 7$) derived by radio-HPLC was (98.77 ± 0.40)% with R_t of 3.33 minutes (Fig. 1A). The RCP was also assessed by radio-PC using ethanol/chloroform/benzene (1.5/2/1.5, v/v/v) and was found to be (99.10 ± 0.66)%, having R_f of 0.59 (Fig. 1B). No activity was found in the solvent front (SF) and point of spotting (POS) ruling out the presence of [^{186}Re]ReO_4^- and [^{186}Re]ReO_2.

A comparative analysis of the radio- and UV-HPLC chromatograms of [^{186}Re]Re-(htbh)$_2$ and its non-radioactive analogue [^{185}Re]Re-(htbh)$_2$ confirms the formation of the

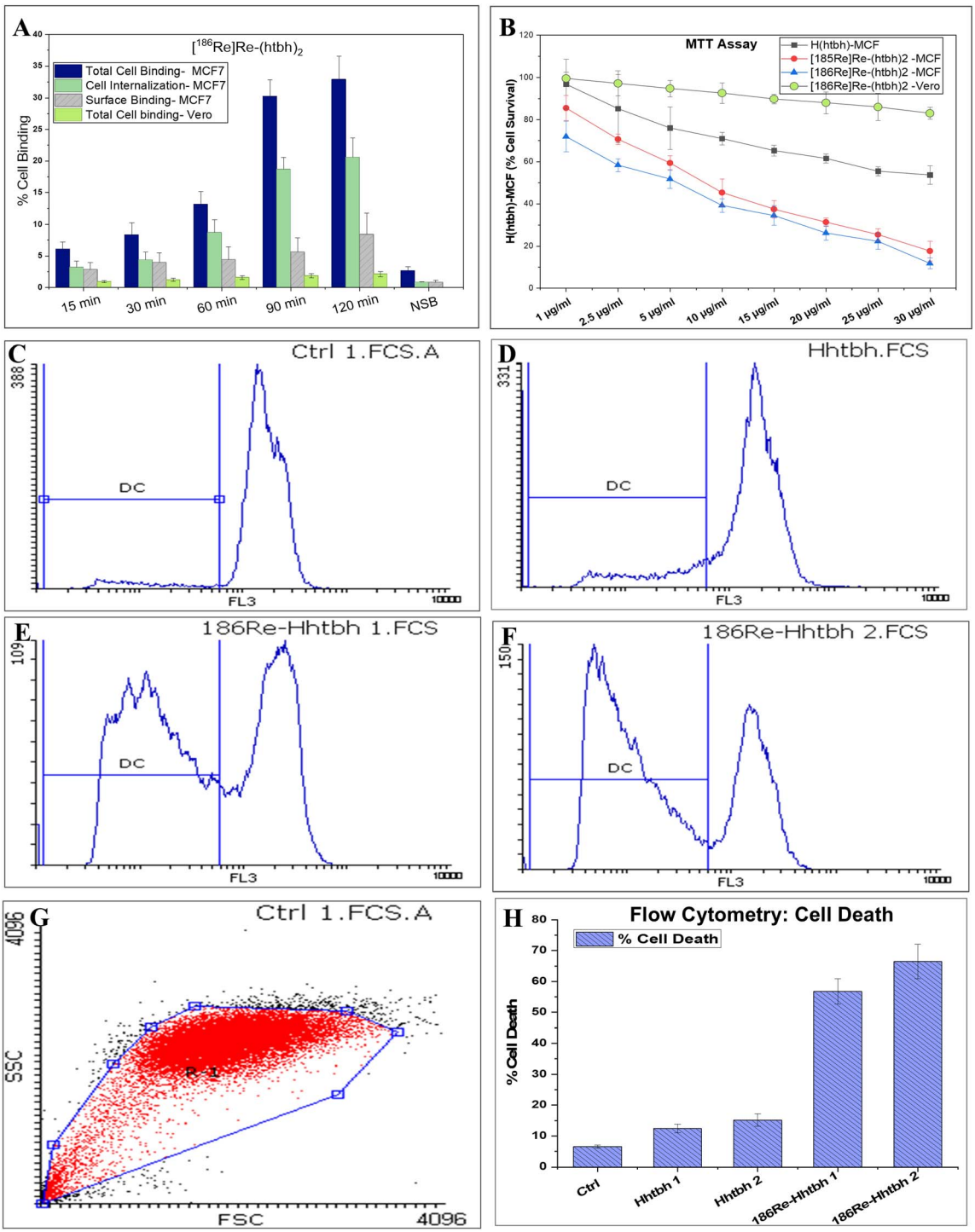

Fig. 2 (A): Cell binding, cell internalization and surface bound–[^{186}Re]Re-(htbh)$_2$ in MCF7 and Vero cell line; (B): MTT-based Cytotoxicity of H(htbh) and [^{186}Re]Re-(htbh)$_2$ in MCF7 and Vero cell line, showing comparative cell viability following pulsed treatment; Flow Cytometry-based detection of percentage sub G1 or dead cell population (DC) in (C): Control MCF 7 cells; and in treatment groups including (D): H(htbh); (E): [^{186}Re]Re-(htbh)$_2$–Group 1; (F): [^{186}Re]Re-(htbh)$_2$–Group 2. (G): Setting for live and dead cell selection using FSC and SSC plot; and (H): histogram showing percentage of dead cell population (DC) in different treatment groups.

^{186}Re-labeled complex. This is evidenced by the close retention times of the radioactive peak at 3.33 minutes (Fig. 1A) and the UV-detected peak of the non-radioactive complex at 3.20 minutes (Fig. 1E). For validating the radio-HPLC method, the [^{186}Re]Re-(htbh)$_2$ was spiked with known concentration of [^{186}Re]ReO_4^-. Radio-HPLC chromatogram (Fig. 1F) exhibits two peaks with R_t 3.52 and 2.62 minutes corresponding to [^{186}Re]Re-(htbh)$_2$ and [^{186}Re]ReO_4^- respectively.

3.3 Stability and transchelation studies results of [^{186}Re]Re-(htbh)$_2$ complex

3.3.1 Saline stability. The retention of RCP values of (98.01 ± 0.47)%, up to 3 h, on storage, at 25 °C (room temperature), using 2,5-dihydroxybenzoic acid as stabilizer, with RAC of ~107 MBq mL^{-1} as observed from radio-HPLC chromatogram (R_t: 3.52 minutes, Fig. 1C, $n = 7$), were indicative of the *in-vitro* saline stability of the [^{186}Re]Re-(htbh)$_2$ complex.

3.3.2 PBS stability. The RCP of the [^{186}Re]Re-(htbh)$_2$ complex was found to be (98.27 ± 0.37)% up to 24 h, post-incubation in PBS at 37 °C using radio-HPLC. The complex stability was further confirmed by radio-HPLC of the complex, post incubation in PBS showing distinct single radioactive peak (Fig. 1G, $n = 3$) having R_t of 3.33 minutes.

3.3.3 Serum stability. Radio-PC chromatogram of the complex in serum samples, post-storage (at −20 °C up to 18 h) exhibit a clear and distinct single radioactive peak (Fig. 1D, $n = 7$) with R_f of 0.52, (solvent system: ethanol/chloroform/benzene: 1.5/2/1.5, v/v/v) thus establishing the RCP to be > 98%.

3.3.4 Transchelation/ligand exchange. Transchelation studies, were carried out post 24 h incubation of the [^{186}Re]Re-(htbh)$_2$ complex, at 37 °C along with DTPA (100 fold molar excess of Re). The RCP of the complex was found to be (98.09 ± 0.11)% using radio-HPLC. The stability was further confirmed by radio-HPLC of [^{186}Re]Re-(htbh)$_2$, post incubation, with excess DTPA wherein a distinct single radioactive peak (Fig. 1H, $n = 3$) at R_t of 3.42 minutes was observed. This confirmed the stability of the complex [^{186}Re]Re-(htbh)$_2$ in the presence of challenging ligands.

The specific activity of [^{186}Re]Re-(htbh)$_2$ complex ($n = 7$) was found to be 187.11 MBq μmole^{-1}. The EL of [^{186}Re]Re-(htbh)$_2$ was found to be < 25 EU mL^{-1} ($n = 7$) with sterility remaining intact for all the produced batches.

3.4 Characterization studies of [^{185}Re]Re-(htbh)$_2$ complex

3.4.1 HRMS. The formation of the complex was confirmed by HRMS using LCMS-QTOF method. The HRMS spectrum exhibits a characteristic isotopic cluster at m/z 516.9941, 518.9960, 519.9989, 520.9924, and 521.9921 corresponding to the calculated mass of $C_{14}H_{14}N_4O_2{}^{185}Re_1S_2$.

3.4.2 FT-IR data (powder form, ν, cm^{-1}). 3100–3300 (br, νO–H), 3055 (br, νN–H), 1611 (νC = N), 1577 (δN–H), 1455 (νC–N), 1153 (νC = S), 746 (νC–S), 564 (νRe–S), 445 (νRe–N). Notably, no absorption band is observed in the 950–1000 cm^{-1} region corresponding to ν(Re=O).

3.4.3 ^{1}H NMR (400 MHz, $CDCl_3$ δ ppm). 11.15 (s, phenolic OH), 7.56 (d, $J = 7.8$ Hz Aromatic), 7.43 (t, $J = 7.9$ Hz, Aromatic), 7.15 (d, $J = 8.4$ Hz, Aromatic), 7.00 (t, $J = 7.5$ Hz, Aromatic).

3.5 *In-vitro* pharmacokinetic studies of [^{186}Re]Re-(htbh)$_2$

3.5.1 Cell binding and internalization studies. *In-vitro* cell binding and cell internalization analyses of [^{186}Re]Re-(htbh)$_2$ were carried out in MCF7 cells. The results showed a specific binding of (32.01 ± 3.66)% (Fig. 2A). A sizeable fraction of the cell-bound [^{186}Re]Re-(htbh)$_2$ (20.59 ± 3.07)% gets internalized into the MCF7 cells, upon 2 h of incubation (Fig. 2A). A significant reduction in specific bindings were observed on pre-incubation with 100 nM of cold H(htbh) (0.82 ± 0.33)%. This ascertains the specificity of [^{186}Re]Re-(htbh)$_2$ for the cell surface antigens. Non-specific binding studies performed using Vero cells (non-cancerous African green monkey kidney cells) showed minimal and weakly time-dependent binding, with total cell binding remaining below (2.14 ± 0.42)% even at 120 min (Fig. 2A), indicating negligible non-specific interaction.

3.5.2 *In vitro* cytotoxic potency of [^{186}Re]Re-(htbh)$_2$. The cytotoxic potential of free H(htbh) and [^{186}Re]Re-(htbh)$_2$ was evaluated in MCF-7 cells using a colorimetric MTT assay, with vehicle-treated cells as controls. As shown in Fig. 2B, treatment of MCF-7 cells with [^{186}Re]Re-(htbh)$_2$ resulted in a clear concentration-dependent reduction in metabolically active viable cells, corresponding to increasing ^{186}Re-associated radioactive dose at higher ligand-equivalent concentrations.

Following 24 h incubation, [^{186}Re]Re-(htbh)$_2$ produced pronounced cytotoxicity, with cell viability decreasing from 71.9 ± 7.3% at 1 μg mL^{-1} (~1.1 MBq mL^{-1}) to 11.8 ± 0.6% at 30 μg mL^{-1} (~33.5 MBq mL^{-1}). A significant loss of viability was observed at 10 μg mL^{-1} (~11.1 MBq mL^{-1}) (39.2 ± 1.2%) and 20 μg mL^{-1} (~22.3 MBq mL^{-1}) (26.2 ± 0.4%), confirming a strong dose–response relationship ($P < 0.001$).

The free H(htbh) ligand showed minimal cytotoxicity, with cell viability remaining 96.8 ± 11.7% at 1 μg mL^{-1} and 28.7 ± 9.1% at 30 μg mL^{-1}.

To assess non-specific toxicity, the MTT assay was also performed in Vero (non-cancerous) cells, where [^{186}Re]Re-(htbh)$_2$ maintained high cell viability (>83%) even at 30 μg mL^{-1} (~33.42 MBq mL^{-1}), indicating low off-target cytotoxicity. Collectively, these results demonstrate that the observed dose-dependent cytotoxicity in MCF-7 cells is predominantly driven by ^{186}Re-associated radioactivity, with minimal contribution from the ligand alone. Results are expressed as mean ± SD ($n = 3$).

3.5.3 Flow cytometry based cytotoxicity studies of [^{186}Re]Re-(htbh)$_2$. Flow cytometry-based analysis was carried out to determine the efficacy of [^{186}Re]Re-(htbh)$_2$ on inducing apoptotic/necrotic cell death in breast cancer cell line MCF-7, as compared with unlabeled H(htbh) at an equivalent dose. In our study, the necrotic and apoptotic cell subset with fragmented DNA were depicted as Sub-G1 cell population in Propidium iodide-based flow cytometry analysis. From Fig. 2C–F, it was observed that the percentage of Sub G1 cells were significantly higher in [^{186}Re]Re-(htbh)$_2$ 10 and 20 μg mL^{-1} treatment group (58.1% and 66.18% respectively) as compared to H(htbh) 10 and 20 μg mL^{-1} (12.05%). The percentage of Sub G1 cells in vehicle control group was 6.42%. This is apparent from the flow histogram that [^{186}Re]Re-(htbh)$_2$ has higher potential to induce cytotoxicity and apoptotic cell death in breast cancer cell line, MCF7, as compared to an equivalent dose of the unlabeled H(htbh).

Fig. 2G and H depicts the graphical representation of flow cytometry-based cell population selected for analysis and histogram of cell cytotoxicity analysis in MCF7 cell line by PI staining respectively. Cells were incubated for 24 h with

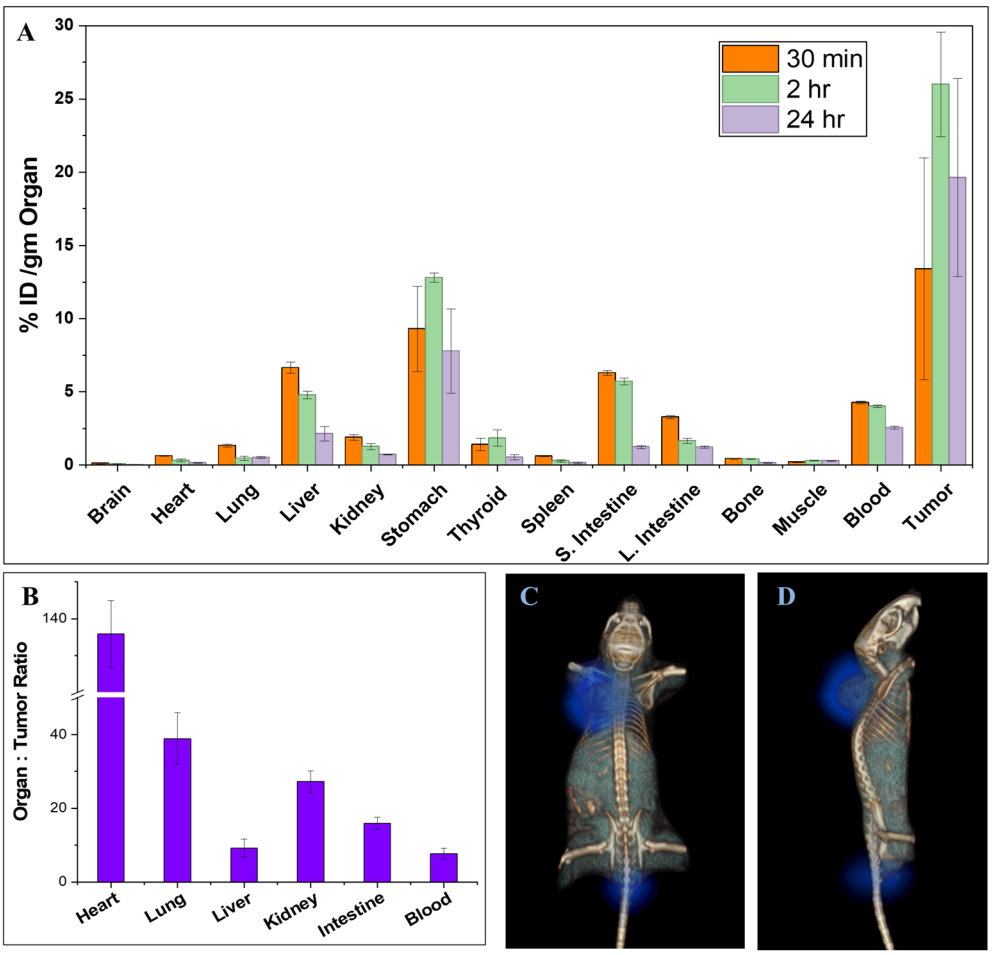

Fig. 3 (A): Biodistribution of [^{186}Re]Re-(htbh)$_2$ in MCF-7 tumour xenografted female SCID mice; (B): tumour to organ ratio, 2 h post injection; (C and D): SPECT/CT images of female SCID mice with MCF7 tumour xenograft.

different H(htbh) formulations including H(htbh) (10 μg mL^{-1} and 20 μg mL^{-1}), [^{186}Re]Re-(htbh)$_2$ (10 μg mL^{-1} and 20 μg mL^{-1}), and vehicle control. The "*Y*" axis represents the cell number and the "*X*" axis represents the cellular DNA content as fluorescence intensity of the PI dye.

3.6 *In-vivo* distribution studies of [^{186}Re]Re-(htbh)$_2$

A significant degree of tumour-specific uptake of [^{186}Re]Re-(htbh)$_2$ was observed in *in-vivo* distribution study, using tumour-xenografted mice model (Fig. 3A). Considerable retention of the complex was seen in the tumour induced with MCF7 cell lines. Maximum accumulation in MCF7 xenograft tumour (25.99 ± 3.55)% ID g^{-1} was observed at 2 h p.i, with nominal depletion at latter time points. There were no reported studies on the uptake pattern of [^{186}Re]Re-(htbh)$_2$ in cell line xenograft. Moderate accumulation of the complex was observed in other major organs including in the kidneys (1.27 ± 0.21)% ID/g and liver (4.76 ± 0.26)% ID g^{-1}, at 2 h post injection, which showed progressive clearance with time *via* the renal route. Minimal accumulation of activity was seen in other organs, at 2 h post-administration which gradually reduced with time (24 h). Notably, a measurable degree of gastric uptake was observed, which is consistent with the known physiological behavior of perrhenate {[^{186}Re]ReO_4^-), a substrate of the sodium–iodide symporter (NIS) expressed in gastric mucosa. Literature reports indicate that perrhenate exhibits prominent early uptake in stomach and salivary tissues, followed by partial washout over time. In the present study, although stomach uptake was evident, it did not show a sustained increasing trend at later time points. Furthermore, thyroid uptake remained low and non-progressive across time points.[43] Together, these findings suggest that any *in vivo* reoxidation of [^{186}Re]Re-(htbh)$_2$ is limited and transient, and does not lead to significant systemic release of free perrhenate.

The radioactivity in blood was high at initial time points (4.02 ± 0.08)% ID g^{-1} at 2 h which cleared with time (2.55 ± 0.09%) ID g^{-1} at 24 h. Relatively less uptake in other major organs with respect to HER-2 expressing tumour is also presented in Fig. 3A. Histogram of tumour-to-organ ratios in tumour-xenografted mice, 2 h post injections are depicted in Fig. 3B.

The SPECT/CT analyses revealed uptake of the [^{186}Re]Re-(htbh)$_2$ complex in the MCF7 xenografted tumour of female SCID mice at 2 h p.i. as well as clearance from the plasma by

24 h (Fig. 3C and D). Moderately low amount of radioactivity was present in the liver and bladder, at longer time points. The findings from the imaging studies are in agreement with the *in-vivo* distribution study in mice.

3.7 Optimization of the radiolabeling process

3.7.1 Metal to ligand ratios. In order to maximize the RCY of the final product, [^{186}Re]Re-(htbh)$_2$, an optimization of metal to ligand molar ratios is one of the important requirement, while using non-carrier free, medium specific activity [^{186}Re]ReO_4^- (specific activity ranging from 9.99–10.28 GBq mg^{-1}). Hence, the radiolabeling was carried out with three different metal {[^{186}Re]Re(VII)} to ligand [H(htbh)] molar ratios, *viz.* (1 : 6, 1 : 8 and 1 : 10). The highest RCY and RCP of [^{186}Re]Re-(htbh)$_2$ was observed (Fig. 4A) on carrying out the radiolabeling at 1 : 10 metal to ligand ratios.

3.7.2 pH of [^{186}Re]ReO_4^-. Though rhenium and technetium have similar chemical properties by virtue of being in the same group of the periodic table, reduction of rhenium complexes are comparatively difficult, since these complexes are kinetically inert for ligand substitution.[44] While radiolabeling with [^{99m}Tc]TcO_4^- are generally carried out at pH between 5-6, the radiolabeling of ligands with $^{186/188}$Re must be achieved at a lower pH of [$^{188/186}$Re]ReO_4^- in the range of 1–2.[44] In the present study, the radiolabeling of H(htbh) with [^{186}Re]ReO_4^- was carried out at pH 2, which resulted in highest RCY and RCP of (97.04 ± 0.49)% and (98.77 ± 0.40)% respectively. However, on carrying out the radiolabeling at pH 5–6, the RCY and RCP of the [^{186}Re]Re-(htbh)$_2$ complex was < 70% as seen from Fig. 4B. The low RCP could be attributed to the higher pH, wherein the redox potential of Sn^{2+}/Sn^{4+} ion is low. However, at pH of ~2, the reduction of [^{186}Re]ReO_4^- increases thereby facilitating the maximum complexation, resulting in > 98% RCP of the [^{186}Re]Re-(htbh)$_2$ complex.[45,46]

3.7.3 Incubation temperature and time. During the initial optimization of the radiolabeling protocol, reactions were carried out at 100 °C for 5 min. In addition, radiolabeling was also attempted at lower temperatures (25 °C and 50 °C) to evaluate the effect of temperature on complex formation.

At 100 °C (5 min), the formation of [^{186}Re]Re-(htbh)$_2$ was confirmed by radio-PC and radio-HPLC analyses. The radio-PC chromatogram exhibited a single distinct peak with an R_f value of 0.59 (Fig. 1B), while radio-HPLC showed a single radioactive peak at R_t = 3.33 min (Fig. 1A). Further confirmation was obtained from the UV-HPLC chromatogram of the non-radioactive analogue {[^{185}Re]Re-(htbh)$_2$}, which displayed a corresponding UV-active peak at R = 3.20 min (Fig. 1E).

In addition to chromatographic characterization, both radioactive and non-radioactive complexes exhibited a faint green colour; however, such visual observations were regarded as supplementary and interpreted in conjunction with radio-PC and radio-HPLC data.

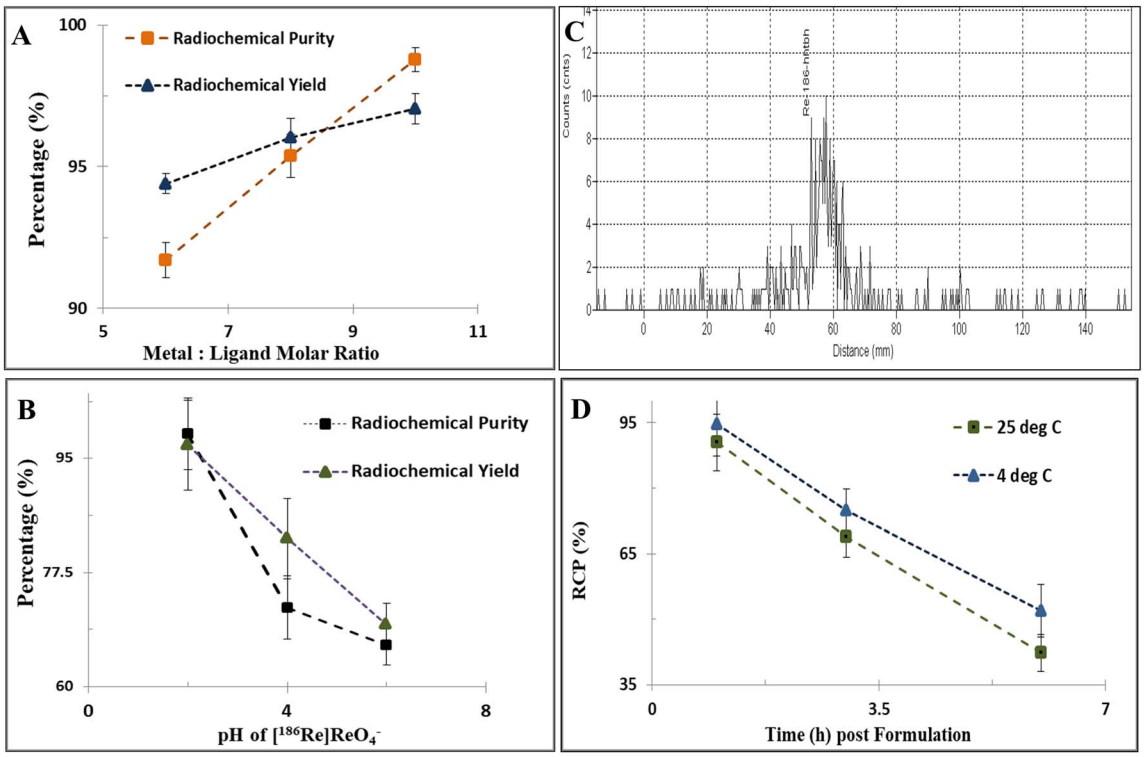

Fig. 4 Influence of (A): metal (Re): ligand [H(htbh)] molar ratio; (B): [^{186}Re]ReO_4^- pH on radiochemical purity (RCP) and radiochemical yield (RCY) of [^{186}Re]Re-(htbh)$_2$; (C): radio-PC of [^{186}Re]Re-(htbh)$_2$ in ethanol/chloroform/benzene (1.5/2/1.5, v/v/v) solvent system, showing the degradation of the product (shift in R_f from 0.59 to 0.85) under the influence of prolonged incubation time (10 min) at 100 °C; and (D): influence of storage temperature on RCP of [^{186}Re]Re-(htbh)$_2$ up to 6 h post formulation without gentisic acid.

Radiolabeling at 25 °C and 50 °C also resulted in formation of the desired complex, as indicated by radio-PC ($R_f \approx 0.50$–0.60; data not shown), along with similar faint green colouration. However, significantly longer incubation times (~90 min at 25 °C and ~40 min at 50 °C) were required, indicating slower reaction kinetics. These conditions were therefore not considered suitable for standardization of the radiolabeling protocol.

To investigate the stability of the complex under prolonged heating, the reaction was also carried out at 100 °C for 10 min. Under these conditions, the radio-PC chromatogram exhibited a single peak with a shifted R_f value of 0.85 (Fig. 4C), indicating the formation of a different radiochemical species. Concurrently, the solution became colourless, suggesting transformation or degradation of the initially formed complex.

This observation is consistent with literature reports that Re-186 labelled thiohydrazide-based complexes generally retain their core structure at elevated temperatures for short durations; however, prolonged heating can lead to decomposition, possibly through loss of coordinated or associated water molecules and subsequent weakening or cleavage of ligand coordination bonds.[47]

3.7.4 *In vitro* stability of [^{186}Re]Re-(htbh)$_2$. The [^{186}Re]Re-(htbh)$_2$ (RAC of the complex was ~107 MBq mL^{-1}) was found to be stable up to 24 h post formulation on incubation at 37 °C in PBS, in presence of gentisic acid (3.1 mg GBq^{-1}). The *in-vitro* saline stability of [^{186}Re]Re-(htbh)$_2$ complex was also investigated at three different time points (1 h, 2 h and 3 h), post formulation, at room temperature without any stabilizing agent. The radio-PC (solvent: ethanol/chloroform/benzene, 1.5/2/1.5, v/v/v) chromatogram showed the formation of [^{186}Re]ReO_4^- *via* reoxidation of Re(III) and also the presence of reduced/hydrolyzed Re in the form of [^{186}Re]ReO_2 in the product. The amount of [^{186}Re]ReO_4^- and [^{186}Re]ReO_2 species in the product was found to increase with time in absence of any stabilizer (Fig. 4D) due to radiolysis.[48]

The observations indicate that in absence of a stabilizer, the Re(III) centre in the [^{186}Re]Re-(htbh)$_2$ complex is not stabilized by complexation with the H(htbh) ligand and reoxidation takes place leading to the formation of [^{186}Re]ReO_4^- and [^{186}Re]ReO_2 species. This can be attributed to possible multiple bonds formation between nitrogen and oxygen in its +3 oxidation state.[49] However, the formation of such multiple bonds could be restricted by adding a suitable stabilizer (gentisic acid), in appropriate concentration.

4 Discussion

4.1 Quality control of the radiochemical precursor [^{186}Re]ReO_4^- used for radiolabeling

Despite the similarities in chemical properties of [^{99m}Tc]TcO_4^- and [^{186}Re]ReO_4^- by virtue of their periodic analogies, an inherent challenge involved in the development of ^{186}Re based radiopharmaceuticals is that the rhenium complexes require more stringent conditions for their preparation and that the Re complexes have a higher tendency to get reoxidized to perrhenate than the analogous technetium complexes.[50] Hence it becomes essential to use [^{186}Re]ReO_4^- sourced from the reactor, in its purest form, free from any oxidizing impurities which are generated from different radiochemical species, if any, present in the [^{186}Re]ReO_4^-. Generally different radiochemical species in the [^{186}Re]ReO_4^- are generated during the 4 d cooling period of $^{186/188}$Re, post irradiation in the reactor. However such radiochemical species in the [^{186}Re]ReO_4^- are eliminated by suitable methods of optimization, radiochemical separation and purification.[39,50]

The enriched ^{185}Re target (enrichment: >95%) on irradiation, produces ^{186}Re ($t_{1/2}$: 90.64 h) *via* ^{185}Re(n,γ)^{186}Re nuclear reaction. However, small quantity of ^{188}Re ($t_{1/2}$: 16.98 h) was also co-produced *via* ^{187}Re(n,γ)^{188}Re nuclear reaction during the irradiation of enriched ^{185}Re, due to existence of ^{187}Re in the target material. The presence of ^{188}Re in the [^{186}Re]ReO_4^- form, therefore constitutes a major radionuclide impurity which cannot be eliminated by any optimized radiochemical separation and purification process. Hence, a 4 d cooling of the irradiated target was required to eliminate the radionuclide impurity of ^{188}Re < 1% in the produced [^{186}Re]ReO_4^-.[50,51]

Prior to radiolabeling of H(htbh) ligand with [^{186}Re]ReO_4^-, the RCP of the precursor radiochemical *viz.* [^{186}Re]ReO_4^- was evaluated. This was necessary since the irradiated target was subjected to 4 d cooling before radiochemical separation and purification. In order to rule out the presence of any other radiochemical species in [^{186}Re]ReO_4^- which might interfere during radiolabeling with H(htbh) ligand, the RCP evaluation was carried out by radio-TLC in saline. The RCP of the [^{186}Re]ReO_4^- precursor was estimated to be ~99% (observed activity at R_f 0.98) with insignificant activity at the POS.

4.2 Characterization of [^{185}Re]Re-(htbh)$_2$ complex

On the basis of the combined FT-IR, NMR and HRMS data, the ligand *ortho*-hydroxythiobenzhydrazide provides a suitable multidentate coordination environment capable of stabilising reduced rhenium centers, leading to the formulation of Re complex coordinated by two ligand molecules.

The mode of coordination of H(htbh) in the rhenium complex has been inferred from its known coordination behaviour and from spectroscopic evidence obtained in the present study. Complexation was carried out under acidic conditions, under which deprotonation of the phenolic –OH group is not favoured. Consistent with this, the phenolic –OH proton is clearly observed in the ^{1}H NMR spectrum at δ 11.15 ppm and the corresponding ν(O–H) stretching vibration (br 3100–3300 cm^{-1}) is retained in the FT-IR spectrum, indicating that the phenolic oxygen does not participate in metal coordination. The ligand therefore coordinates to the rhenium centre predominantly through the hydrazide nitrogen and the thioamide sulphur donor atoms, forming a N,S-chelate. Owing to the equilibrium between the two forms of the donor array R–C(=S)–NH–NH_2 (Form A) ↔ R–C(SH)=N–NH_2 (Form B),[28] present in the ligand H(htbh) the coordination of [^{185}Re]Re metal for the "Form A" (Fig. 5C) takes place involving coordinate bond with = S and covalent bond with NH_2, while for the "Form B" (Fig. 5C) the coordination of [^{185}Re]Re metal takes place involving a covalent bond with SH and coordinate bond

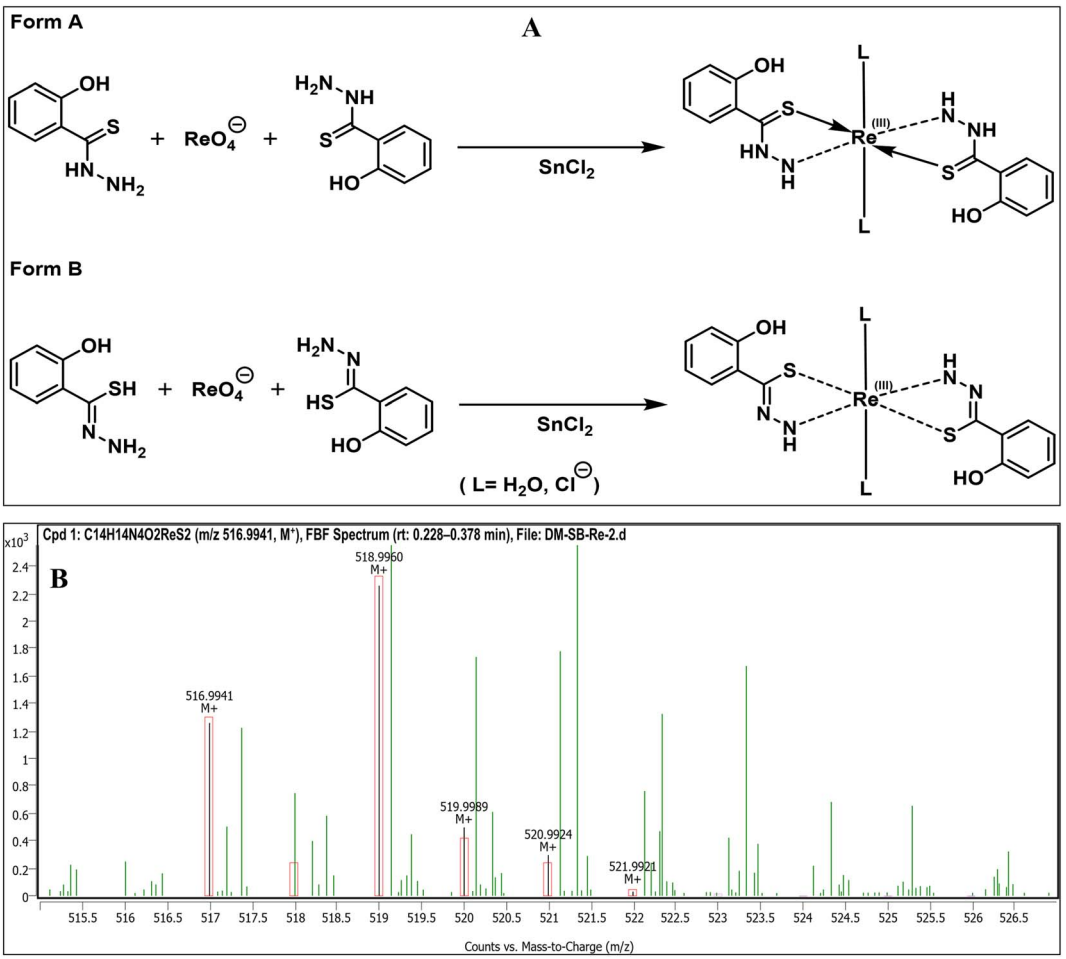

Fig. 5 (A): Two possible bonding modes of Re, with Forms A and B of the ligand H(htbh), resulting in the two forms of [^{185}Re]Re-(htbh)$_2$; (B): HRMS spectrum of [^{185}Re]Re-(htbh)$_2$ complex, exhibiting prominent molecular ion peaks (*m*/*z* 516.9941, 518.9960 and 520.9924).

with NH_2.[52,53] The FT-IR spectrum of the complex shows the complete absence of the characteristic ν(Re═O) stretching vibration (expected at 960–1000 cm^{-1}), confirming that the (Re═O) core is absent in the complex. The other bands *viz.* 1611 (νC = N), 1577 (δN–H), 1455 (νC–N), 1153 (νC = S), 746 (νC–S), 564 (νRe–S), 445 (νRe–N), observed in the FT-IR spectrum also support the speculated mode of coordination. Reduction of perrhenate during radiolabeling in the presence of $SnCl_2$ is therefore inferred to generate rhenium in a lower oxidation state, most plausibly Re(III), in agreement with reported rhenium chemistry under similar conditions. Comparable Re(III) complexes featuring N,S-donor ligands and solvent or water completed octahedral coordination spheres have been reported[54,55] in the rhenium coordination chemistry literature, supporting the structural assignment proposed here. Such a structure is favourable for both *in-vivo* stability and target engagement, as chelation through hard-soft donor combinations creates a robust coordination sphere around the metal.

Based on the Q-TOF HRMS data, the complex is best described as having a coordinated Re(III) centre in which two ligands bind through N and S donor atoms, while the remaining coordination sites are likely occupied by solvent molecules and/or coordinated water. The proposed structure (Fig. 5A) is consistent with this coordination description and is supported by the available spectroscopic data.

The proposed mode of complexation is supported by Q-TOF HRMS analysis of the non-radioactive [^{185}Re]Re-(htbh)$_2$ complex ($C_{14}H_{14}N_4O_2{}^{185}ReS_2$). The spectrum exhibits a prominent molecular ion peak at *m*/*z* 518.9960, corresponding to [^{185}M]$^+$, along with a peak at *m*/*z* 519.9989 assigned to the protonated species [^{185}M + H]$^+$. In addition, a peak at *m*/*z* 516.9941, attributed to the doubly deprotonated species [^{185}M–2H]$^{2-}$, was observed. The formation of such ions in Q-TOF HRMS is commonly influenced by solvent polarity, analyte concentration, and instrumental parameters such as cone voltage.[56,57]

Additional peaks at *m*/*z* 520.9924 ([^{187}M]$^+$) and 521.9921 ([^{187}M + H]$^+$) were also detected, consistent with the natural isotopic distribution of rhenium (^{185}Re: 37.40%; ^{187}Re: 62.60%). The ~2 unit mass shift relative to the corresponding ^{185}Re peaks confirms the contribution of the ^{187}Re isotope.

Overall, the HRMS data are consistent with the formation of [Re(htbh)$_2$], comprising two coordinated H(htbh) ligands. Although single-crystal X-ray diffraction would be required for definitive structural elucidation, the structure proposed in Fig. 5A represents the most plausible arrangement supported by the available spectroscopic data.

Notably, no solvent- or water-coordinated species were observed in the mass spectrum. This is expected, as HRMS measurements are performed under high vacuum, where weakly coordinated solvent molecules are readily dissociated during ionization.[58] Furthermore, the orthogonal sampling interface of Q-TOF instruments limits the transmission of solvent clusters into the mass analyser.[59]

4.3 *In-vitro* pharmacokinetic studies of $[^{186}Re]Re-(htbh)_2$

The biological relevance of the structural characteristics of the resulting $[^{186}Re]Re-(htbh)_2$ complex, particularly its stability and potential lipophilicity conferred by the aromatic thiobenzyl moiety, may favour its passive accumulation and retention in tumour tissue,[60] while the presence of hydrazide functionality may also allow for specific interactions with biomolecular targets overexpressed in malignant cells.

The present study highlights the potential of $[^{186}Re]Re-(htbh)_2$ as a selective radiolabeled agent for breast cancer targeting. The *in-vitro* binding and internalization studies in MCF7 cells demonstrated efficient and specific uptake of $[^{186}Re]Re-(htbh)_2$, with minimal non-specific interaction in non-cancerous Vero cells. Competitive inhibition with unlabeled H(htbh) confirmed receptor-mediated binding, underscoring its specificity towards receptor overexpression in breast cancer cells. The cytotoxic efficacy of $[^{186}Re]Re-(htbh)_2$ was evident from MTT assays, where the radiolabeled formulation was found to significantly reduce MCF7 cell viability, while the unlabeled H(htbh) exhibited negligible cytotoxicity. Flow cytometry-based analysis further revealed substantial apoptotic cell death induced by $[^{186}Re]Re-(htbh)_2$, as reflected by the marked increase in Sub-G1 cell population compared to controls. *In-vivo* biodistribution and SPECT/CT imaging studies corroborated these findings, demonstrating preferential tumour accumulation of $[^{186}Re]Re-(htbh)_2$ with sustained retention up to 24 hours. Favourable tumour-to-organ ratios and clearance *via* renal pathways further support its potential for targeted radiotherapy. Minimal off-target accumulation in non-target organs such as liver and kidneys indicates a promising safety profile. Notably, a measurable degree of gastric uptake was observed, consistent with the known physiological behavior of perrhenate $\{[^{186}Re]ReO_4^-\}$ *via* sodium–iodide symporter (NIS)-mediated transport in gastric mucosa. However, the absence of a progressive increase in gastric uptake, together with low and non-progressive thyroid accumulation, indicates that any *in vivo* reoxidation of $[^{186}Re]Re-(htbh)_2$ is limited and transient.[43] Collectively, these results establish $[^{186}Re]Re-(htbh)_2$ as a promising agent for targeted radionuclide therapy of breast cancer, warranting further preclinical evaluation.

It is well documented that high specific activity of $[^{186}Re]ReO_4^-$ (111–148 GBq mg^{-1}) is a pre-requisite for formulation of multiple clinical therapeutic doses (single patient dose: ~2.8 GBq) of any $[^{186}Re]Re$ based complexes *viz.* $[^{186}Re]Re$-HEDP, $[^{186}Re]Re$-BMEDA, $[^{186}Re]Re$-bivatuzumab.[22] However, the primary aim of our work was to evaluate the specificity of the complex $[^{186}Re]Re-(htbh)_2$ towards targeting the overexpressed receptors in MBC. Hence, we carried out the radiolabeling of H(htbh) with $[^{186}Re]ReO_4^-$ having medium to low specific activity of ~10 GBq mg^{-1}.

5 Conclusion

In conclusion, we report the successful development of a robust and reproducible radiolabeling strategy for the aromatic thiobenzhydrazide derivative, *o*-hydroxythiobenzhydrazide, using $[^{186}Re]ReO_4^-$ to yield the stable complex $[^{186}Re]Re-(htbh)_2$. The radiocomplex demonstrates high radiochemical purity and stability, along with favourable biological characteristics, including significant cytotoxicity and binding affinity in MCF-7 cells. Notably, *in vivo* evaluation in MCF7-induced xenograft models revealed sustained and selective tumour accumulation, as confirmed by SPECT/CT imaging.

Collectively, these findings highlight the potential of $[^{186/188}Re]Re-(htbh)_2$ as a promising radiotheranostic agent for metastatic breast cancer, combining diagnostic capability with therapeutic relevance. Importantly, the optimized radiolabeling protocol is readily translatable to $[^{188}Re]$, thereby facilitating its broader clinical applicability. Overall, this study provides compelling preclinical evidence supporting further investigation and development of this radiocomplex toward targeted radionuclide therapy of metastatic breast cancer.

Author contributions

A. M. performed radiolabeling of H(htbh) with $[^{186}Re]ReO_4$, physicochemical and biological quality control of $[^{186}Re]Re-(htbh)_2$, synthesis and characterization of the cold $[^{185}Re]Re$ complex, and made the first draft of the manuscript. A. C. conducted the *in-vitro* and *in-vivo* studies of $[^{186}Re]Re-(htbh)_2$ and wrote the related manuscript sections. T. U. carried out SPECT/CT imaging of tumour-xenografted SCID mice. S. S. standardized and validated radio-HPLC methods. M. T. performed culture work of MCF7 and other cell lines. S. C., R. C., and K. V. V. produced ^{186}Re from enriched ^{185}Re targets, processed and purified it to $[^{186}Re]ReO_4^-$. S. K. conducted and recorded ^1H-NMR spectra of $[^{185}Re]Re-(htbh)_2$. D. S. and S. G. (Snigdha Gangopadhyay) carried out the chemical synthesis of the ligand, S. G. (Sanchita Goswami) provided the resources and arranged for funding from CSIR for carrying out the studies related to synthesis and characterization of the cold ligand. S. G. (Sanchita Goswami), S. G. (Snigdha Gangopadhyay) and P. K. G. jointly conceived the work. S. B. conceptualized the project and the overall radioactive studies, led the project, ensured isotope availability, provided resources and overall administrative oversight, and reviewed and edited the final manuscript.

Conflicts of interest

There are no conflicts of interest to declare.

Data availability

All data supporting the findings of this study are included within the article. Raw datasets underlying the analyses are

available from the corresponding author upon reasonable request. Source data are provided with this manuscript to facilitate transparency and reproducibility.

Acknowledgements

The authors sincerely thank the staff of the Hospital Radiopharmacy Section, Scintigraphy Section and the Animal House Facility of the Radiation Medicine Centre, Bhabha Atomic Research Centre (BARC), for providing the necessary facilities to carry out this work. The assistance of Professor D. Maiti, Department of Chemistry, IIT Bombay, in acquiring HRMS data is gratefully acknowledged. We also thank Bio-Organic Division, BARC, for providing the FT-IR data. The authors also acknowledge the support and encouragement of the Director, Medical Group, BARC. One of the authors, Sanchita Goswami acknowledges the support from CSIR [Sanction No.: 01(2869)/17/EMR-II] and is thankful to DST-FIST, DST-PURSE, and CAS(V) of the Department of Chemistry, University of Calcutta, for access to instrumental facilities, required for synthesis of the non-radioactive ligand.

Notes and references

1 B. A. Güleç and F. Yurt, Treatment with Radiopharmaceuticals and Radionuclides in Breast Cancer: Current Options, *Eur. J. Breast Health*, 2021, **17**(3), 214, DOI: 10.4274/EJBH.GALENOS.2021.2021-3-4.

2 S. R. Mehta, V. Suhag, M. Semwal and N. Sharma, Radiotherapy: Basic Concepts and Recent Advances, *Med. J. Armed Forces India*, 2010, **66**(2), 158–162, DOI: 10.1016/S0377-1237(10)80132-7.

3 G. Sgouros, L. Bodei, M. R. McDevitt and J. R. Nedrow, Radiopharmaceutical therapy in cancer: clinical advances and challenges, *Nat. Rev. Drug Discov.*, 2020, **19**(9), 589–608, DOI: 10.1038/s41573-020-0073-9.

4 L. Marcu, E. Bezak and B. J. Allen, Global comparison of targeted alpha vs targeted beta therapy for cancer: In vitro, in vivo and clinical trials, *Crit. Rev. Oncol.-Hematol.*, 2018, **123**, 7–20, DOI: 10.1016/J.CRITREVONC.2018.01.001.

5 A. Musket, S. Davern, B. M. Elam, P. R. Musich, J. P. Moorman and Y. Jiang, The application of radionuclide therapy for breast cancer, *Front. Nucl. Med.*, 2023, **3**, 1323514, DOI: 10.3389/FNUME.2023.1323514/BIBTEX.

6 A. Chakraborty, A. Mitra, S. Sahu, *et al.*, Intricacies in the Preparation of Patient Doses of [^{177}Lu]Lu-Rituximab and [^{177}Lu]Lu-Trastuzumab Using Low Specific Activity [^{177}Lu]LuCl3: Methodological Aspects, *Mol. Imaging Biol.*, 2024, **26**(1), 61–80, DOI: 10.1007/S11307-023-01846-1/METRICS.

7 G. L. Ray, K. E. Baidoo, L. M. M. Keller, P. S. Albert, M. W. Brechbiel and D. E. Milenic, Pre-Clinical Assessment of ^{177}Lu-Labeled Trastuzumab Targeting HER2 for Treatment and Management of Cancer Patients with Disseminated Intraperitoneal Disease, *Pharmaceuticals*, 2012, **5**(1), 1–15, DOI: 10.3390/ph5010001.

8 N. Vinod, J. H. Kim, S. Choi and I. Lim, Combination of ^{131}I-trastuzumab and lanatoside C enhanced therapeutic efficacy in HER2 positive tumour model, *Sci. Rep.*, 2021, **11**(1), 12871, DOI: 10.1038/S41598-021-92460-0.

9 E. W. Price, K. J. Edwards, K. E. Carnazza, *et al.*, A comparative evaluation of the chelators H4octapa and CHX-A″-DTPA with the therapeutic radiometal ^{90}Y, *Nucl. Med. Biol.*, 2016, **43**(9), 566–576, DOI: 10.1016/J.NUCMEDBIO.2016.06.004.

10 P. Krcisz, K. Czarnecka, L. Królicki, E. Mikiciuk-Olasik and P. Szymański, Radiolabeled Peptides and Antibodies in Medicine, *Bioconjug. Chem.*, 2021, **32**(1), 25–42, DOI: 10.1021/ACS.BIOCONJCHEM.0C00617.

11 B. Mitran, S. S. Rinne, M. W. Konijnenberg, *et al.*, Trastuzumab cotreatment improves survival of mice with PC-3 prostate cancer xenografts treated with the GRPR antagonist ^{177}Lu-DOTAGA-PEG2 -RM26, *Int. J. Cancer*, 2019, **145**(12), 3347–3358, DOI: 10.1002/IJC.32401.

12 S. Hermanto, R. D. Haryuni, M. Ramli, A. Mutalib and S. Hudiyono, Synthesis and stability test of radioimmunoconjugate ^{177}Lu-DOTA-F(ab′)2-trastuzumab for theranostic agent of HER2 positive breast cancer, *J. Radiat. Res. Appl. Sci.*, 2016, **9**(4), 441–448, DOI: 10.1016/J.JRRAS.2016.07.001.

13 S. Hermanto, R. Dini, H. Badan, *et al.*, Preparation of F (ab') 2 trastuzumab fragment for Radioimmunoconjugate synthesis of 177 Lu-DOTA-F (ab') 2-trastuzumab, *IOSR J. Pharm.*, 2024, **2**, 12–18. https://www.iosrphr.org.

14 W. Roll, M. Müther, G. Böning, *et al.*, First clinical experience with fractionated intracavitary radioimmunotherapy using [^{177}Lu]Lu-6A10-Fab fragments in patients with glioblastoma: a pilot study, *EJNMMI Res.*, 2023, **13**(1), 78, DOI: 10.1186/S13550-023-01029-7.

15 B. Altunay, A. Morgenroth, M. Beheshti, *et al.*, HER2-directed antibodies, affibodies and nanobodies as drug-delivery vehicles in breast cancer with a specific focus on radioimmunotherapy and radioimmunoimaging, *Eur. J. Nucl. Med. Mol. Imaging*, 2021, **48**(5), 1371–1389, DOI: 10.1007/S00259-020-05094-1.

16 M. D'Huyvetter, C. Vincke, C. Xavier, *et al.*, Targeted radionuclide therapy with A ^{177}Lu-labeled anti-HER2 nanobody, *Theranostics*, 2014, **4**(7), 708–720, DOI: 10.7150/THNO.8156.

17 Y. Rathore, T. Lakhanpal, S. Chakraborty, *et al.*, Targeting Breast Cancer Using ^{177}Lu-Labeled Trastuzumab and Trastuzumab Fragment : First-in-Human Clinical Experience, *Clin. Nucl. Med.*, 2024, **49**(6), E258–E265, DOI: 10.1097/RLU.0000000000005208.

18 M. D'Huyvetter, A. Aerts, C. Xavier, *et al.*, Development of ^{177}Lu-nanobodies for radioimmunotherapy of HER2-positive breast cancer: evaluation of different bifunctional chelators, *Contrast Media Mol. Imaging*, 2012, **7**(2), 254–264, DOI: 10.1002/CMMI.491.

19 F. J. Daha, S. Rasaneh and S. S. Zahabi, Preparation of ^{177}Lu-Rituximab and Comparison with 131I-Rituximab Radiolabeled with Chloramine-T Method, *J. Clin. Res. Paramed. Sci.*, 2018, **72**(2), 87181, DOI: 10.5812/JCRPS.87181.

20 L. Zhao, J. Gong, Q. Qi, *et al.*, ^{131}I-Labeled Anti-HER2 Nanobody for Targeted Radionuclide Therapy of HER2-Positive Breast Cancer, *Int. J. Nanomed.*, 2023, **18**, 1915–1925, DOI: 10.2147/IJN.S399322.

21 M. Ramli, B. Hidayat, S. Sutari, S. Setyowati and V. Y. Susilo, Rituximab Iodination Procedure for Radioiodinated Rituximab (^{131}I-Rituximab) Preparation, *Maj. Kedokt. Bdg.*, 2019, **51**(2), 95–103, DOI: 10.15395/MKB.V51N2.1595.

22 B. Altunay, A. Goedicke, H. Oliver, O. H. Winz, *et al.*, ^{99m}Tc-labeled single-domain antibody for SPECT/CT assessment of HER2 expression in diverse cancer types, *Eur. J. Nucl. Med. Mol. Imaging*, 2023, **50**(4), 1005–1013, DOI: 10.1007/s00259-022-06066-3.

23 P. T. Acharya, Z. A. Bhavsar, D. J. Jethava, D. B. Patel and H. D. Patel, A review on development of bio-active thiosemicarbazide derivatives: Recent advances, *J. Mol. Struct.*, 2021, **1226**, 129268, DOI: 10.1016/J.MOLSTRUC.2020.129268.

24 R. A. Finch, M. C. Liu, S. P. Grill, *et al.*, Triapine (3-aminopyridine-2-carboxaldehyde- thiosemicarbazone): A potent inhibitor of ribonucleotide reductase activity with broad spectrum antitumour activity, *Biochem. Pharmacol.*, 2000, **59**(8), 983–991, DOI: 10.1016/S0006-2952(99)00419-0.

25 B. H and G. D, The wide pharmacological versatility of semicarbazones, thiosemicarba-zones and their metal complexes, *Mini Rev. Med. Chem.*, 2004, **4**(1), 31–39, DOI: 10.2174/1389557043487484.

26 B. Kaproń, A. Płazińska and W. Płaziński, Identification of the First-In-Class Dual Inhibitors of Human DNA Topoisomerase IIα and Indoleamine-2,3-Dioxygenase 1 (Ido 1) with Strong Anticancer Properties, *J. Enzyme Inhib. Med. Chem.*, 2023, **38**(1), 192–202, DOI: 10.1080/14756366.2022.2140420.

27 B. Kaproń, R. Czarnomysy, D. Radomska, K. Bielawski and T. Plech, Thiosemicarbazide Derivatives Targeting Human TopoIIα and IDO-1 as Small-Molecule Drug Candidates for Breast Cancer Treatment, *Int. J. Mol. Sci.*, 2023, **24**(6), 5812, DOI: 10.3390/IJMS24065812.

28 P. Basak, S. Gangopadhyay, S. De, M. G. B. Drew and P. K. Gangopadhyay, Cobalt(III) complexes of some aromatic thiohydrazides – Synthesis, characterization and structure, *Inorg. Chim. Acta*, 2010, **363**(7), 1495–1499, DOI: 10.1016/J.ICA.2010.01.011.

29 D. Sengupta, S. Gangopadhyay, S. Goswami, *et al.*, Novel Low Spin Mixed Ligand Thiohydrazide Complexes of Iron(III): Synthesis, Spectral Characterization, Molecular Modeling, and Antibacterial Activity, *Int. J. Inorg. Chem.*, 2014, **2014**, 1–9, DOI: 10.1155/2014/580232.

30 D. Sengupta, S. Gangopadhyay, M. G. B. Drew and P. K. Gangopadhyay, Thiohydrazide complexes of molybdenum and their relevance to reduction of dinitrogen to ammonia, *Dalton Trans.*, 2014, **44**(3), 1323–1331, DOI: 10.1039/C4DT01945H.

31 S. Argibay-Otero, L. Gano, C. Fernandes, A. Paulo, R. Carballo and E. M. Vázquez-López, Chemical and biological studies of Re(I)/Tc(I) thiosemicarbazonate complexes relevant for the design of radiopharmaceuticals, *J. Inorg. Biochem.*, 2020, **203**, 110917, DOI: 10.1016/J.JINORGBIO.2019.110917.

32 E. Schiller, S. Seifert, F. Tisato, *et al.*, Mixed-Ligand Rhenium-188 Complexes with Tetradentate/Monodentate NS3/P ('4 + 1') Coordination: Relation of Structure with Antioxidation Stability, *Bioconjug. Chem.*, 2005, **16**(3), 634–643, DOI: 10.1021/BC049745A.

33 Q. Qi, Q. Wang, Y. Li, *et al.*, Recent Development of Rhenium-Based Materials in the Application of Diagnosis and Tumour Therapy, *Molecules*, 2023, **28**(6), 2733, DOI: 10.3390/MOLECULES28062733.

34 Radiological Data: Rhenium-186, https://ehs.missouri.edu/sites/ehs/files/pdf/isotopedata/re-186.pdf. Accessed February 8, 2005.

35 M. Argyrou, A. Valassi, M. Andreou and M. Lyra, Rhenium-188 production in hospitals, by w-188/re-188 generator, for easy use in radionuclide therapy, *Int. J. Mol. Imaging*, 2013, **2013**, 1–7, DOI: 10.1155/2013/290750.

36 S. Todde, P. K. Peitl, P. Elsinga, *et al.*, Guidance on validation and qualification of processes and operations involving radiopharmaceuticals, *EJNMMI Radiopharm. Chem.*, 2017, **2**(1), 1–29, DOI: 10.1186/S41181-017-0025-9/FIGURES/1.

37 N. Gillings, O. Hjelstuen, J. Ballinger, *et al.*, Guideline on current good radiopharmacy practice (cGRPP) for the small-scale preparation of radiopharmaceuticals, *EJNMMI Radiopharm. Chem.*, 2021, **6**(1), 1–22, DOI: 10.1186/S41181-021-00123-2/TABLES/1.

38 A. J. North, J. A. Karas, M. T. Ma, *et al.*, Rhenium and Technetium-oxo Complexes with Thioamide Derivatives of Pyridylhydrazine Bifunctional Chelators Conjugated to the Tumour Targeting Peptides Octreotate and Cyclic-RGDfK, *Inorg. Chem.*, 2017, **56**, 9725–9741, DOI: 10.1021/acs.inorgchem.7b01247.

39 T. Das, S. Banerjee, G. Samuel, *et al.*, [186/188Re] rhenium-ethylene dicysteine (Re-Ec): preparation and evaluation for possible use in endovascular brachytherapy, *Nucl. Med. Biol.*, 2000, **27**(2), 189–197, DOI: 10.1016/S0969-8051(99)00097-9.

40 S. Gaikwad, A. Chakraborty, S. Salwe, V. Patel, S. Kulkarni and S. Banerjee, Juglone–ascorbic acid synergy inhibits metastasis and induces apoptotic cell death in poorly differentiated thyroid carcinoma by perturbing SOD and catalase activities, *J. Biochem. Mol. Toxicol.*, 2018, **32**, e22176, DOI: 10.1002/jbt.22176.

41 S. R. Menon, A. Mitra and A. Chakraborty, Clinical Dose Preparation of [^{177}Lu]Lu-DOTA-Pertuzumab Using Medium Specific Activity [^{177}Lu]$LuCl_3$ for Radioimmunotherapy of Breast and Epithelial Ovarian Cancers, with HER2 Receptor Overexpression, *Cancer Biother. Radiopharm.*, 2022, **37**(5), 384–402, DOI: 10.1089/CBR.2021.0230.

42 S. Patra, J. Dey and A. Chakraborty, Physicochemical Characterization, Stability, and In Vitro Evaluation of Curcumin-Loaded Solid Lipid Nanoparticles Prepared Using Biocompatible Synthetic Lipids, *ACS Appl. Bio Mater.*, 2023, **6**(7), 2785–2794, DOI: 10.1021/ACSABM.3C00252/SUPPL_FILE/MT3C00252_SI_001.

43 L. S. Zuckier, O. Dohan and Y. Li, Kinetics of Perrhenate Uptake and Comparative Biodistribution of Perrhenate, Pertechnetate, and Iodide by NaI Symporter–Expressing Tissues In Vivo, *J. Nucl. Med.*, 2004, **45**, 500–507.

44 E. Deutsch, K. Libson, J. L. Vanderheyden, A. R. Ketring and H. R. Maxon, The chemistry of rhenium and technetium as related to the use of isotopes of these elements in therapeutic and diagnostic nuclear medicine, *Int. J. Radiat. Appl. Instrum., Part B*, 1986, **13**(4), 465–477, DOI: 10.1016/0883-2897(86)90027-9.

45 K. Horiuchi, H. Saji and A. Yokoyama, Carrier effect on radiolabeling the polynuclear pentavalent rhenium-186 complex of dimercaptosuccinic acid at alkaline pH: 186Re(V)-DMS, *Nucl. Med. Biol.*, 1999, **26**(7), 771–779, DOI: 10.1016/S0969-8051(99)00055-4.

46 J. Singh, K. Reghebi, C. R. Lazarus, *et al.*, Studies on the preparation and isomeric composition of 186Re- and 188Re-pentavalent rhenium dimercaptosuccinic acid complex, *Nucl. Med. Commun.*, 1993, **14**(3), 197–203, DOI: 10.1097/00006231-199303000-00009.

47 A. J. North, J. A. Karas and M. T. Ma, Rhenium and Technetium-oxo Complexes with Thioamide Derivatives of Pyridylhydrazine Bifunctional Chelators Conjugated to the Tumour Targeting Peptides Octreotate and Cyclic-RGDfK, *Inorg. Chem.*, 2017, **56**, 9725–9741, DOI: 10.1021/acs.inorgchem.7b01247.

48 L. Uccelli, M. Petra, M. Pasquali and A. Boschi, Monoclonal Antibodies Radiolabeling with Rhenium-188 for Radioimmunotherapy, *BioMed Res. Int.*, 2017, 1–7, DOI: 10.1155/2017/5923609.

49 J. C. Vites and M. M. Lynam, Rhenium 1996, *Coord. Chem. Rev.*, 1998, **172**(1), 357–388, DOI: 10.1016/S0010-8545(98)00095-2.

50 K. Kothari, M. R. A. Pillai, P. R. Unni, H. H. Shimpi, O. P. D. Noronha and A. M. Samuel, Preparation, stability studies and pharmacological behavior of [^{186}Re]Re–HEDP, *Appl. Radiat. Isot.*, 1999, **51**(1), 51–58, DOI: 10.1016/S0969-8043(98)00195-X.

51 K. Hashimoto, M. Yanis, S. Motoishi', K. Kobayashi and M. Izumo, presented *'Production of 186 Re and 188 Re, and Synthesis of 1M Re-DTPA' at the Proceedings of the 6th Asian Symposium of Research Reactors*, March 29-31, 1999, Japan (JAERI-Conf, 99-006) Session 10-3, JP9950573, pp. 232–237.

52 L. J. Bellamy, *The Infra-red Spectra of Complex Molecules*, Springer, Netherlands, 1975, DOI: 10.1007/978-94-011-6017-9.

53 J. Kleynhans, A. Duatti and C. Bolzati, Fundamentals of Rhenium-188 Radiopharmaceutical Chemistry, *Mol*, 2023, **28**, 1487, DOI: 10.3390/MOLECULES28031487.

54 R. Alberto, R. Schibli, R. Waibel, U. Abram and P. A. Schubiger, Basic aqueous chemistry of $[M(OH_2)_3(CO)_3]^+$ (M=Re, Tc) directed towards radiopharmaceutical applications, *Coord. Chem. Rev.*, 1999, **190–192**, 901–919, DOI: 10.1016/S0010-8545(99)00128-9.

55 J. R. Dilworth and S. J. Parrott, The biomedical chemistry of technetium and rhenium, *Chem. Soc. Rev.*, 1998, **27**(1), 43–55, DOI: 10.1039/A827043Z.

56 M. Franska, A. Zgoła and J. Rychłowska, Formation of $[M–H]^-$ and $[M–2H]^{2-}$ ions in the electrospray ionization mass spectra of dicarboxylated polyethylene glycols, *Rapid Commun. Mass Spectrom.*, 2004, **18**, 356–359, DOI: 10.1002/rcm.1340.

57 N. Zhao, M. Cheng and S. Huang, Various Multicharged Anions of Ginsenosides in Negative Electrospray Ionization with QTOF High-Resolution Mass Spectrometry, *J. Am. Soc. Mass Spectrom.*, 2019, **30**, 403Y418, DOI: 10.1007/s13361-018-2089-5.

58 S. Tamara, M. A. den Boer and A. J. R. Heck, High-Resolution Native Mass Spectrometry, *Chem. Rev.*, 2022, **122**, 7269–7326, DOI: 10.1021/acs.chemrev.1c00212.

59 C. Killeen, A. Kropp and I. C. Chagunda, The amenability of different solvents to electrospray ionization mass spectrometry, *Int. J. Mass Spectrom.*, 2024, **506**, 117349, DOI: 10.1016/j.ijms.2024.117349.

60 B. Fischer, K. Kryeziu, S. Kallus, *et al.*, Nanoformulations of anticancer thiosemicarbazones to reduce methemoglobin formation and improve anticancer activity, *RSC Adv.*, 2016, **6**, 55848, DOI: 10.1039/c6ra07659a.